Spontaneous *in situ* generation of photoemissive aurophilic oligomers in water solution based on the 2-thiocytosine ligand

Daniel Blasco,[a] María Rodríguez-Castillo,[a] M. Elena Olmos,[a] Miguel Monge,[a] and José M. López-de-Luzuriaga.*[a]

[a] Departamento de Química, Centro de Investigación en Síntesis Química (CISQ), Universidad de La Rioja, Madre de Dios 53, 26004 Logroño (Spain).

Electronic Supplementary Information

Table of Contents

1. Instrumentation.

1.1. General procedures.

$[AuCl(PMe_3)]$[1] and Tl(acac)[2] were prepared according to previously published methods. 2-thiocytosine (4-amino-2-mercaptopyrimidine) and silver trifluoroacetate were purchased from Merck and used as received. HPLC grade tetrahydrofuran (THF) was dried and degasified with a MBRAUN SPS-800 solvent purification system. Distilled water was purged with nitrogen for 10 min before photophysical measurements in solution.

1.2. Physical measurements.

^1H ($\delta(SiMe_4)$ = 0.0 ppm), ^{19}F ($\delta(CCl_3F)$ = 0.0 ppm), $^{31}P\{^1H\}$ (δ(85% H_3PO_4) = 0.0 ppm) and $^{13}C\{^1H\}$ ($\delta(SiMe_4)$ = 0.0 ppm) NMR spectra were recorded with a Bruker AVANCE 400 spectrometer ($\nu(^1H)$ = 400 MHz). UATR-IR spectra were recorded with a Perkin-Elmer Spectrum Two spectrophotometer (4000-400 cm^{-1} range, diamond crystal-UATR accessory). ESI-MS spectra were obtained with a Bruker MicroTOF-Q spectrometer. CHNS elemental analyses were carried out with a Perkin-Elmer 240C microanalyser. UV-Vis absorption (quartz cells, optical path = 1 cm) and DRUV-Vis reflectance (diluted with anhydrous KBr) measurements were recorded with a Shimadzu UV-3600 UV-Vis-NIR spectrophotometer. For the latter, a Harrick Praying Mantis accessory was employed, and absorption spectra were calculated following the Kubelka-Munk function. Steady-state luminescence measurements were carried out in a HORIBA Jobin Yvon Fluorolog 3-22 Tau-3 spectrofluorometer. Lifetimes were recorded with a HORIBA Jobin Yvon IBH FluoroHub-B single photon counting system and analyzed with the DAS6 software (employed nanoLEDs: 370, 390, 450 nm). Absolute photoluminescence quantum yields were determined with a Hamamatsu Quantaurus-QY C11347-11 spectrometer from solid samples.

1.3. Crystallography.

Suitable single crystals were mounted in inert oil on MiTeGen micro mounts and transferred to the cold nitrogen stream of a Bruker APEX-II CCD area-detector diffractometer, equipped with an Oxford Instruments low-temperature controller system (Mo Kα = 0.71073 Å, graphite monochromator). Data was collected in ω and ϕ scan mode. Absorption corrections: semiempirical (based on multiple scans). The structure was solved by using direct methods and refined on F^2 with SHELXL.[3] All non-hydrogen atoms were treated anisotropically, and all

[1] K. Angermaier, E. Zeller and H. Schmidbaur, *J. Organomet. Chem.*, 1994, **472**, 371-376.
[2] A. G. Lee, *The Chemistry of Thallium*, Elsevier: New York, 1971.
[3] G. M. Sheldrick, *SHELXL-97, Program for Crystal Structure Refinement*; University of Göttingen: Göttingen, Germany, **1997**.

hydrogen atoms were included as riding bodies. CCDC 2123504 and 21235045 contain the supplementary crystallographic data for this paper. These data can be obtained free of charge via www.ccdc.cam.ac.uk/data_request/cif, or by emailing data_ request@ccdc.cam.ac.uk, or by contacting The Cambridge Crystallographic Data Center, 12 Union Road, Cambridge CB2 1EZ, UK; fax: +44 1223 336033.

1.4. Computational details.

Theoretical calculations were performed with the Gaussian 09 package program.[4] Model systems [Au(*S*-2-thiocytosinate)(PMe_3)] (**2a**) and [{Au(PMe_3)}$_2$(μ-^{1}*N,S*-2-thiocytosinate)]$_2^{2+}$ (**4a**) were built from the X-ray structures of complexes **2** and **4**, respectively, and were completely optimized at the DFT/PBE1PBE level of theory[5] with the third dispersion correction by Grimme (DFT-D3).[6] Model systems [Au_2(μ-*S,N*^{1}-2-thiocytosinate)$_2$]$_2$ (**4b**) and [Au_4(μ-*S,N*^{1}-2-thiocytosinate)$_4$] (**4c**) were built from scratch, and were completely optimized at the DFT/PBE1PBE level of theory with the third dispersion correction by Grimme (DFT-D3) including water in the calculation through a PCM model.

The following basis set combinations were employed: for gold, the quasi-relativistical (QR) 19-valence electrons (VE) pseudopotential (PP) from Andrae[7] and the corresponding basis sets augmented with two *f* polarisation functions were used.[8] Carbon, nitrogen, phosphorus, and sulphur were treated by Stuttgart pseudopotentials,[9] including only the VE for each atom. For these atoms, the double-ζ basis set were used,[10] augmented by *d*-type polarisation functions.[11] For hydrogen, a double-ζ plus a *p*-type polarisation function was used.[11]

Population analyses were calculated with the cclib GaussSum software.[12]

---

[4] *Gaussian 09, Revision D.01*, M.J. Frisch, G.W. Trucks, H.B. Schlegel, G.E. Scuseria, M.A. Robb, J.R. Cheeseman, G. Scalmani, V. Barone, B. Mennucci, G.A. Petersson, H. Nakatsuji, M. Caricato, X. Li, H.P. Hratchian, A.F. Izmaylov, J. Bloino, G. Zheng, J.L. Sonnenberg, M. Hada, M. Ehara, K. Toyota, R. Fukuda, J. Hasegawa, M. Ishida, T. Nakajima, Y. Honda, O. Kitao, H. Nakai, T. Vreven, J.A. Montgomery, Jr., J.E. Peralta, F. Ogliaro, M. Bearpark, J.J. Heyd, E. Brothers, K.N. Kudin, V.N. Staroverov, R. Kobayashi, J. Normand, K. Raghavachari, A. Rendell, J.C. Burant, S.S. Iyengar, J. Tomasi, M. Cossi, N. Rega, J.M. Millam, M. Klene, J.E. Knox, J.B. Cross, V. Bakken, C. Adamo, J. Jaramillo, R. Gomperts, R.E. Stratmann, O. Yazyev, A.J. Austin, R. Cammi, C. Pomelli, J.W. Ochterski, R.L. Martin, K. Morokuma, V.G. Zakrzewski, G.A. Voth, P. Salvador, J.J. Dannenberg, S. Dapprich, A.D. Daniels, Ö. Farkas, J.B. Foresman, J.V. Ortiz, J. Cioslowski, and D.J. Fox, Gaussian, Inc., Wallingford CT, 2009.

[5] J. P. Perdew, K. Burke and M. Ernzerhof, *Phys. Rev. Lett.*, 1996, 77, 3865–3868.

[6] S. Grimme, *Wiley Interdiscip. Rev. Comput. Mol. Sci*., 2011, **1**, 211-228.

[7] D. Andrae, U. Häussermann, M. Dolg, H. Stoll and H. Preuss, *Theor. Chim. Acta*, 1990, **77**, 123-141.

[8] P. Pyykkö, N. Runeberg and F. Mendizabal, *Chem. Eur. J.*, 1997, **3**, 1451-1457.

[9] A. Bergner, M. Dolg, W. Küchle, H. Stoll and H. Preuss, *Mol. Phys.*, 1993, **80**, 1431-1441.

[10] S. Huzinaga, in *Gaussian Basis Sets for Molecular Orbital Calculations*, Elsevier, 1984, p. 16.

[11] S. Huzinaga, *J. Chem. Phys.*, 1965, **42**, 1293-1302.

[12] N. M. O'Boyle, A. L. Tenderholt and K. M. Langner, *J. Comp. Chem.*, 2008, **29**, 839-845.

2. Syntheses of complexes **1-4**.

2.1. Synthesis of [Au(acac)(PMe_3)] (**1**).

A slight excess of Tl(acac) (0.5922 g, 1.92 mmol) is added to a solution of [AuCl(PMe_3)] (0.5000 g, 1.62 mmol) in 20 mL of dichloromethane, which is left to stir protected from direct light overnight (*ca*. 14 h). The ochre suspension of TlCl is filtered over a plug of Celite, which is thoroughly washed with several fractions of dichloromethane, and the resulting transparent yellow filtrate is concentrated *in vacuo* to a volume of *ca*. 2 mL. Addition of 20 mL of *n*-hexane leads to the precipitation of [Au(acac)(PMe_3)] as a brown oil which crystallizes after continuous stirring. Yield: 85 %. ^{1}H NMR (300 MHz, $CDCl_3$) δ/ppm: 4.45-4.41 (1H, d, $^3J_{PH}$ = 12 Hz, CH), 2.29 (6H, s, CH_3), 1.53-1.50 (9H, d, $^2J_{PH}$ = 9 Hz, $P(CH_3)_3$). ^{31}P{^{1}H} NMR (121 MHz, $CDCl_3$) δ/ppm: -1.4 (s, $P(CH_3)_3$). UATR-IR (cm^{-1}): 1629 (C=O). Anal. Calcd. for $C_8H_{16}AuO_2P$: C, 25.82; H, 4.33. Found: C, 26.16; H, 4.01.

2.2. Synthesis of [Au(*S*-2-thiocytosinate)(PMe_3)] (**2**).

An equimolecular amount of 2-thiocytosine (0.0335 g, 0.26 mmol) is added to a suspension of [Au(acac)(PMe_3)] (0.0981 g, 0.26 mmol) in 20 mL of tetrahydrofuran. After 3 h of constant stirring, [Au(*S*-2-thiocytosinate)(PMe_3)] (0.0790 g, 0.20 mmol) is isolated as a yellow solid by filtration of the suspension and further washing with 1 · 10 mL tetrahydrofuran + 1 · 10 mL *n*-hexane. Yield: 75 %. ^{1}H NMR (400 MHz, $(D_3C)_2SO$) δ/ppm: 7.68-7.66 (1H, d,$^3J_{HH}$ = 8 Hz, C^{6}H), 6.40 (2H, bs, NH_2), 5.98-5.96 (1H, d, $^3J_{HH}$ = 6 Hz, C^{5}H), 1.60-1.57 (9H, d, $^2J_{PH}$ = 12 Hz, $P(CH_3)_3$). ^{31}P{^{1}H} NMR (162 MHz, $(D_3C)_2SO$) δ/ppm: -1.2 (s, $P(CH_3)_3$). ^{13}C{^{1}H} NMR (101 MHz, $(D_3C)_2SO$) δ/ppm: 178.77 (s, C^2), 162.84 (s, C^4), 154.90 (s, C^6), 100.24 (s, C^5), 15.62-15.26 (d, $^1J_{PC}$ = 36 Hz, $P(CH_3)_3$). UATR-IR (cm^{-1}): 3391 (NH_2), 3297 (NH_2), 3082 (NH_2). ESI-MS(+) *m/z*: 349.1 ([Au(PMe_3)$_2$]$^+$, calcd. 349.1), 400.0 ([M+H]$^+$, calcd. 400.0), 672.1 ([{Au(PMe_3)}$_2$(μ-*S,N*^{1}-2-thiocytosinate)]$^+$, calcd. 672.0). ESI-MS(-) *m/z*: 449.0 ([Au(*S*-2-thiocytosinate)$_2$]$^-$, calcd. 449.0). Anal. Calcd. for $C_7H_{13}AuN_3PS$: C, 21.06; H, 3.28; N, 10.53; S, 8.03. Found: C, 22.26; H, 3.03; N, 10.64; S, 9.40.

2.3. Synthesis of [Au(*S*-2-thiocytosine)(PMe_3)](CF_3CO_2) (**3**).

An argon protected solution of [AuCl(PMe_3)] (0.1200 g, 0.39 mmol) in 30 mL of dry and degassed THF is cooled to 0 °C in a refrigerating bath. Then, Ag($OCOCF_3$) (0.0862 g, 0.39 mmol) is added to the solution, which is kept under stirring and protected from direct light for 2 hours. After that time, the reaction flask is taken from the bath and opened to air, and the white solid of AgCl is removed by filtration over a plug of Celite. Solid 2-thiocytosine (0.0496 g, 0.39 mmol) is added to the transparent filtrate. After 1 hour of stirring, unreacted 2-thiocytosine and possible coloured by-products are removed by filtration over a plug of Celite, and the colourless filtrate is concentrated *in vacuo* to a volume of *ca.* 2 mL. Addition of 20 mL of diethyl ether leads to the precipitation of [Au(*S*-2-thiocytosine)(PMe_3)](CF_3CO_2) (0.1634 g, 0.32 mmol) as a white solid, which is retrieved from the solution by filtering. Yield: 82 %. ^{1}H NMR (400 MHz, $(D_3C)_2SO$) δ/ppm: 13.36 (bs, SH),8.46-8.29 (m, NH_2 + NH), 7.84-7.83 (1H, d, $^3J_{HH}$ = 8 Hz, C^{6}H), 6.34-6.32 (1H, d, $^3J_{HH}$ = 8 Hz, C^{5}H), 1.67-1.64 (9H, d, $^2J_{PH}$ = 12 Hz, $P(CH_3)_3$). ^{19}F NMR (376 MHz, $(D_3C)_2SO$) δ/ppm: -73.5 (s, $(CF_3CO_2)^-$). ^{31}P{^{1}H} NMR (162 MHz, $(D_3C)_2SO$) δ/ppm: -1.3 (s, $P(CH_3)_3$). ^{13}C{^{1}H} NMR (101 MHz, $(D_3C)_2SO$) δ/ppm: 172.51 (s, C^2), 163.23 (s, C^4), 158.52-158.21 (m, CO_2), 144.27 (s, C^6), 122.29-113.33 (q, $^1J_{CF}$ = 302 Hz, CF_3), 100.86 (s, C^5), 15.17-14.79 (d, $^1J_{PC}$ = 38 Hz, $P(CH_3)_3$). UATR-IR (cm^{-1}): 3316 (NH_2), 3114 (NH_2), 1627 (C=O). ESI-MS(+) *m/z*: 349.1 ([Au(PMe_3)$_2$]$^+$, calcd. 349.1), 400.0

([M]$^+$, calcd. 400.0), 672.1 ([{Au(PMe_3)}$_2$(μ-*S,N*^{1}-2-thiocytosinate)]$^+$, calcd. 672.0). ESI-MS(-) *m/z*: 449.0 ([Au(*S*-2-thiocytosinate)$_2$]$^-$, calcd. 449.0). Λ_M (CH_3OH): 80.9 $cm^2 \cdot \Omega^{-1} \cdot mol^{-1}$. Anal. Calcd. for $C_9H_{14}AuF_3N_3O_2PS$: C, 21.06; H, 2.75; N, 8.19; S, 6.25. Found: C, 23.82; H, 2.69; N, 9.89; S, 8.86.

2.4. Synthesis of [{Au(PMe_3)}$_2$(μ-*S,N*^{1}-2-thiocytosinate)](CF_3CO_2) (**4**).

An equimolecular amount of [Au(acac)(PMe_3)] (**1**, 0.0720 g, 0.19 mmol) is added to a solution of [Au(*S*-2-thiocytosine)(PMe_3)](CF_3CO_2) (**3**, 0.1000 g, 0.19 mmol) in 20 mL of tetrahydrofuran. After 3 h of constant stirring, the suspension is concentrated *in vacuo* to a volume of *ca*. 2 mL, when 20 mL of diethyl ether are added. The white solid of [{Au(PMe_3)}$_2$(μ-*S,N*^{1}-2-thiocytosinate)(PMe_3)](CF_3CO_2) (0.1244 g, 0.16 mmol) is retrieved from the solution by filtering. Yield: 84 %. ^{1}H NMR (400 MHz, CD_3OD) δ/ppm: 7.77-7.76 (1H, d, $^3J_{HH}$ = 4 Hz, ^{6}CH), 6.31-6.30 (1H, d, $^3J_{HH}$ = 4 Hz, ^{5}CH), 1.72-1.69 (18H, d, $^2J_{PH}$ = 12 Hz, P(CH_3)$_3$). ^{19}F NMR (376 MHz, CD_3OD) δ/ppm: -76.9 (s, (CF_3CO_2)$^-$). ^{31}P{^{1}H} NMR (162 MHz, CD_3OD) δ/ppm: -9.0 (s, P(CH_3)$_3$). UATR-IR (cm^{-1}): 3318 (NH_2), 3092 (NH_2), 1690 (C=O). ESI-MS(+) *m/z*: 349.1 ([Au(PMe_3)$_2$]$^+$, calcd. 349.1), 400.0 ([Au(*S*-2-thiocytosine)(PMe_3)]$^+$, calcd. 400.0), 672.0 ([M]$^+$, calcd. 672.0). ESI-MS(-) *m/z*: 113.0 ([CF_3CO_2]$^-$, calcd. 113.0). Λ_M (CH_3OH): 83.2 $cm^2 \cdot \Omega^{-1} \cdot mol^{-1}$. Anal. Calcd. for $C_{12}H_{22}Au_2F_3N_3O_2P_2S$: C, 18.35; H, 2.82; N, 5.35; S, 4.08. Found: C, 18.40; H, 2.85; N, 5.30; S, 4.04.

3. Spectroscopic characterization of complexes **1-4**.

3.1. UATR-IR spectra.

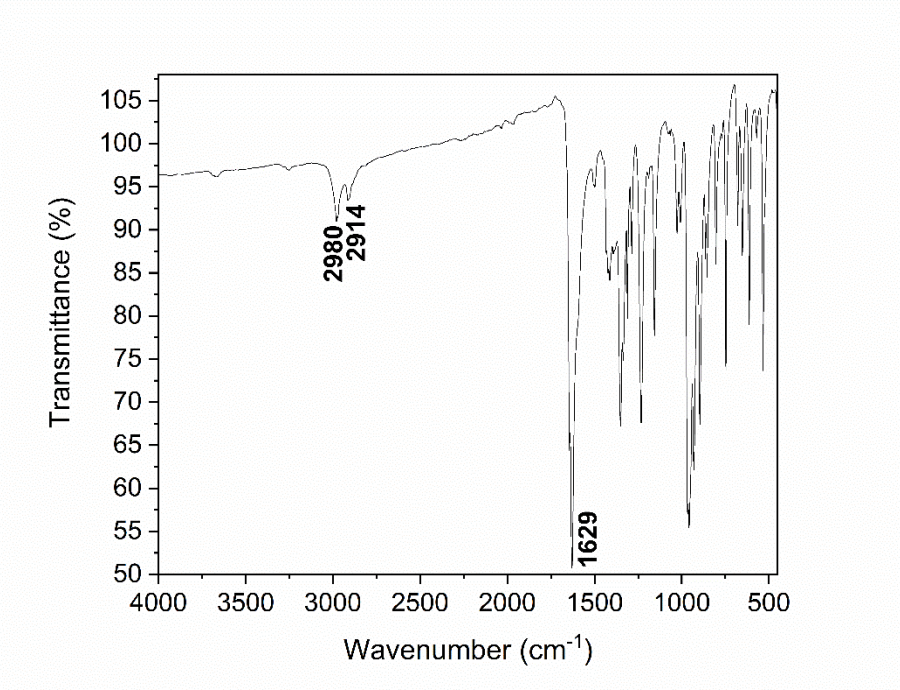

Figure S1. UATR-IR spectrum of [Au(acac)(PMe_3)] (**1**).

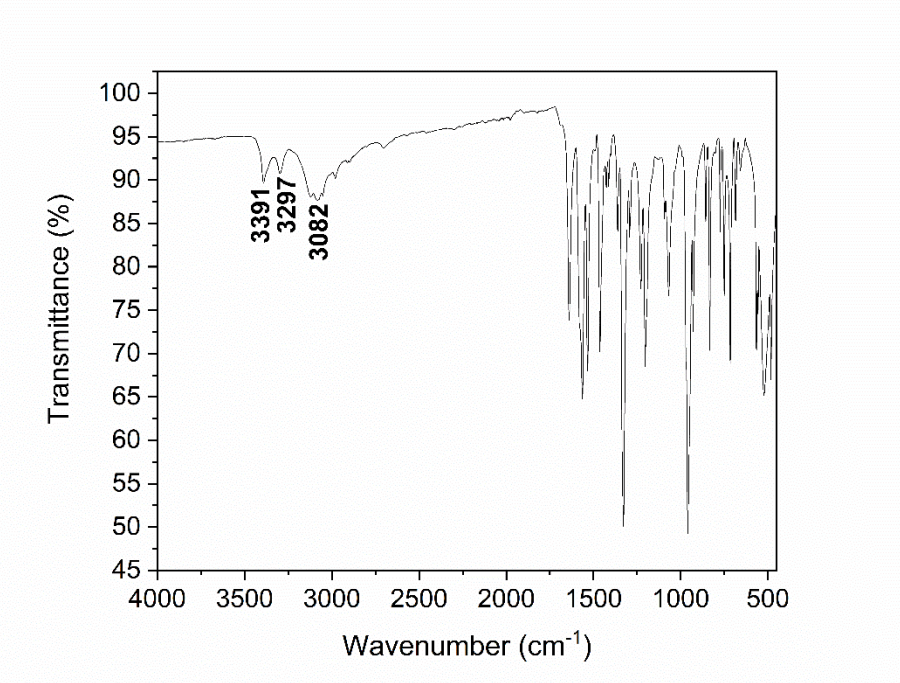

Figure S2. UATR-IR spectrum of [Au(*S*-2-thiocytosinate)(PMe_3)] (**2**).

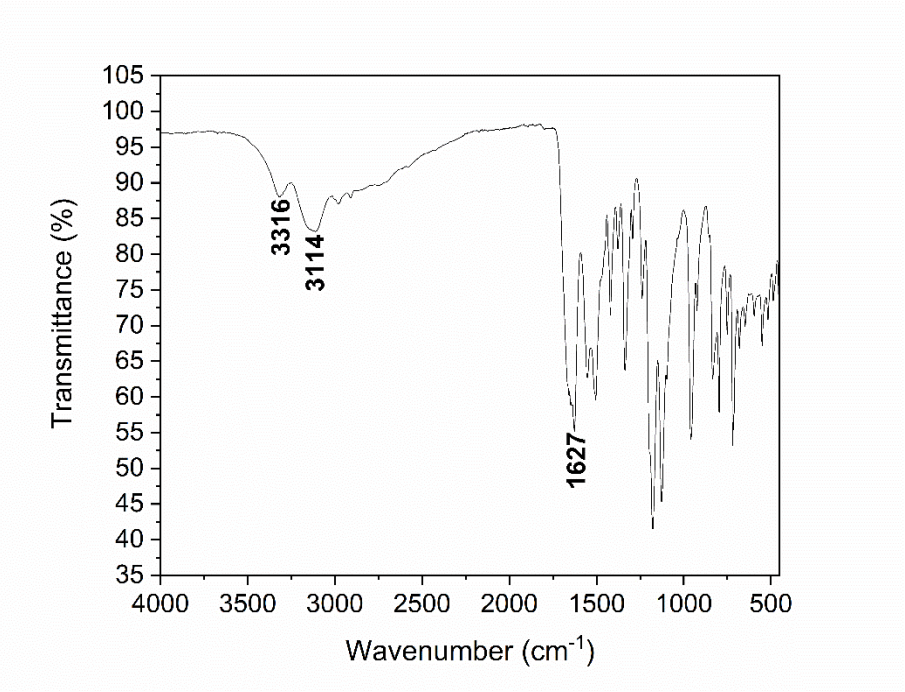

Figure S3. UATR-IR spectrum of [Au(*S*-2-thiocytosine)(PMe_3)](CF_3CO_2) (**3**).

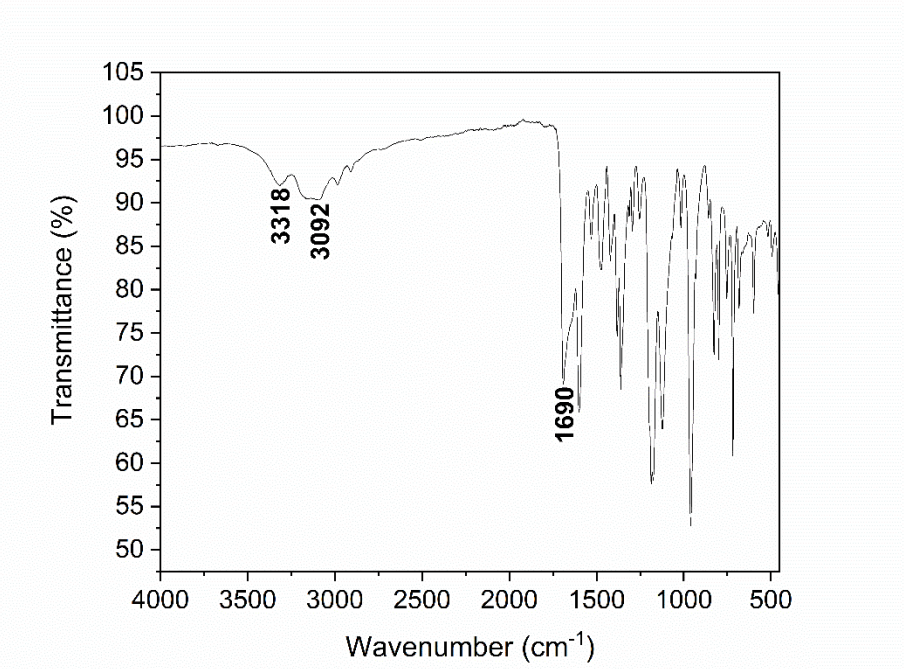

Figure S4. UATR-IR spectrum of [{Au(PMe_3)}$_2$(μ-*S*,N^1-2-thiocytosinate)(PMe_3)](CF_3CO_2) (**4**).

3.2. ^{1}H and $^{31}P\{^{1}H\}$ NMR spectra of [Au(acac)(PMe_3)] (**1**).

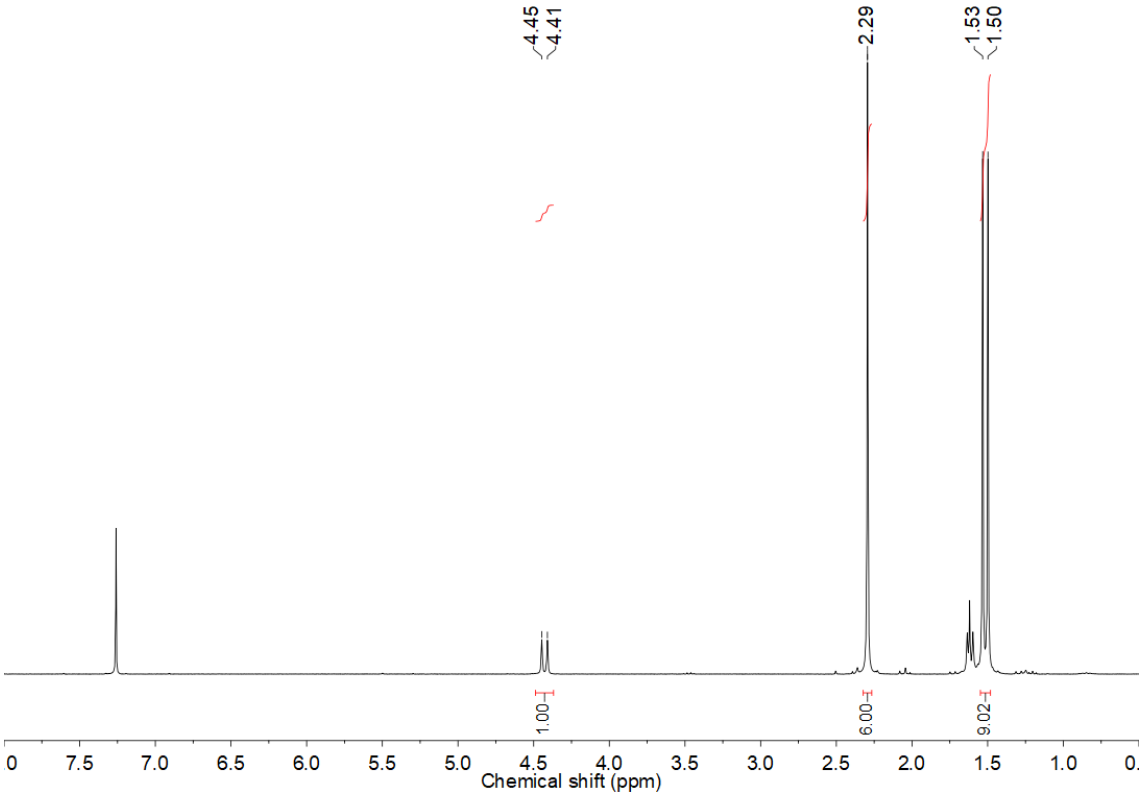

Figure S5. ^{1}H (300 MHz, $CDCl_3$) NMR spectrum of [Au(acac)(PMe_3)] (**1**).

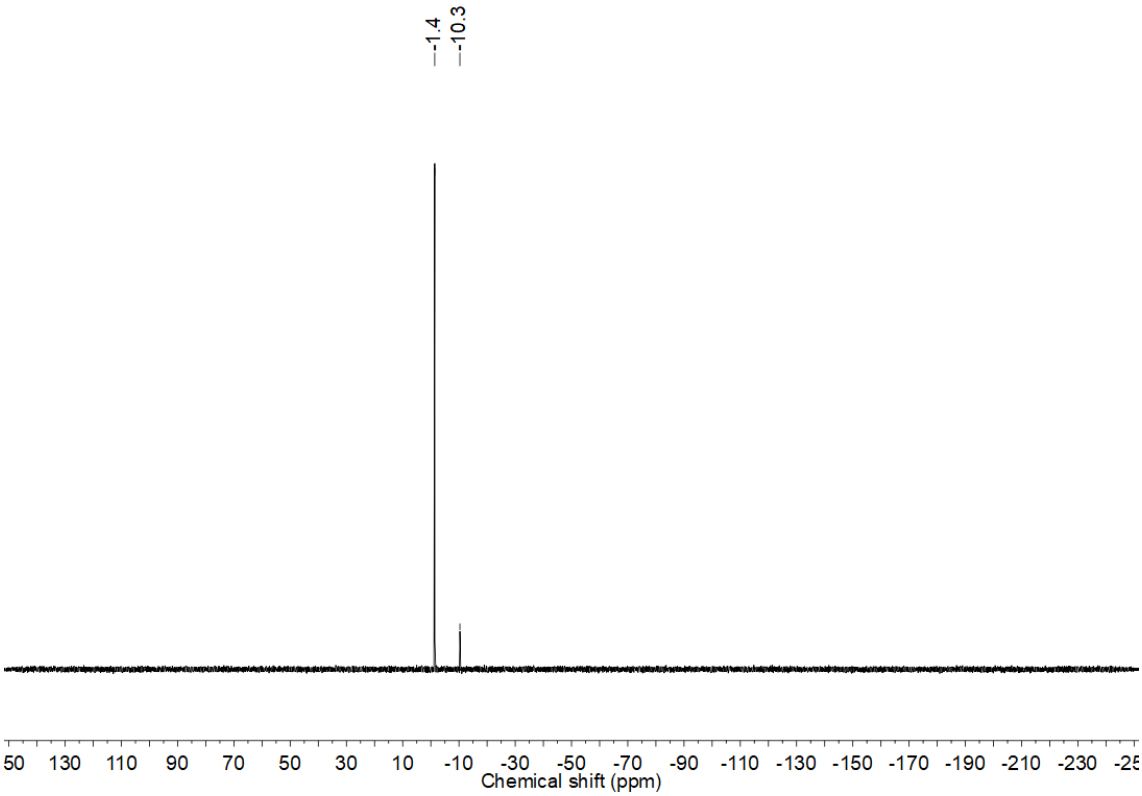

Figure S6. $^{31}P\{^{1}H\}$ (121 MHz, $CDCl_3$) NMR spectrum of [Au(acac)(PMe_3)] (**1**). The minor peak at -10.3 ppm corresponds to unreacted [AuCl(PMe_3)].

3.3. ^{1}H, $^{31}P\{^{1}H\}$ and $^{13}C\{^{1}H\}$ NMR spectra of [Au(*S*-2-thiocytosinate)(PMe_3)] (**2**).

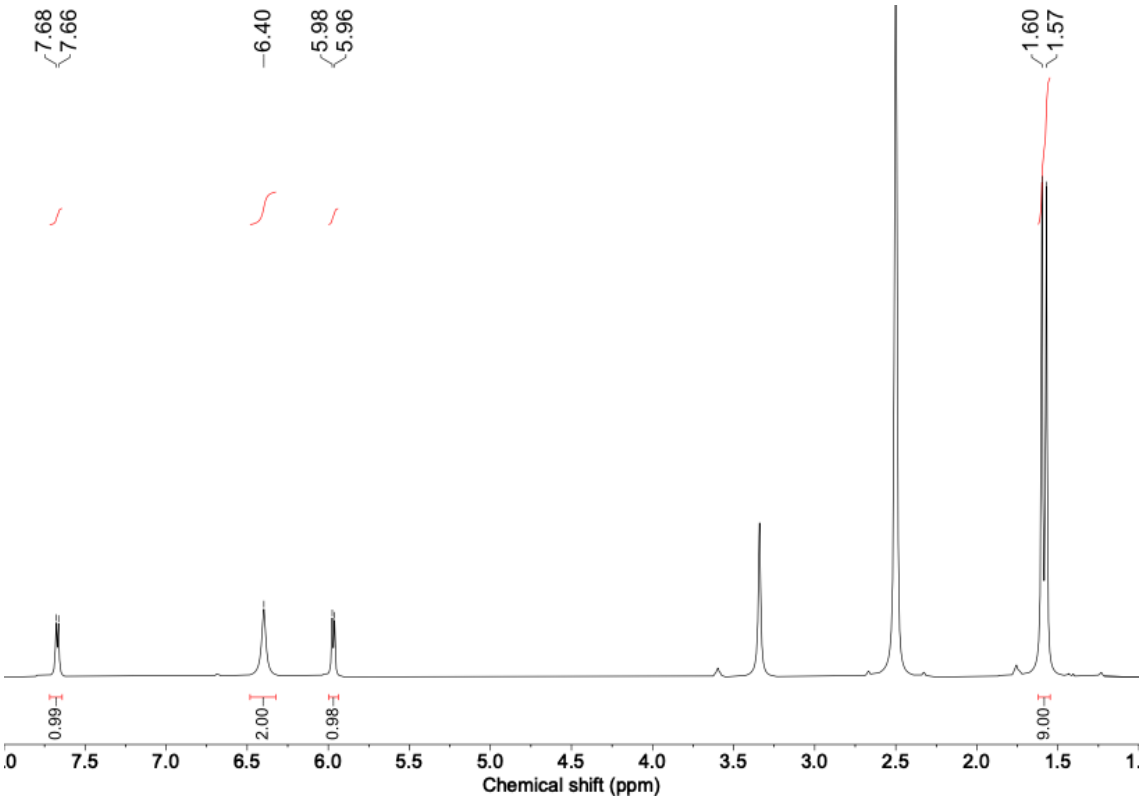

Figure S7. ^{1}H (400 MHz, $(D_3C)_2SO$) NMR spectrum of [Au(*S*-2-thiocytosinate)(PMe_3)] (**2**).

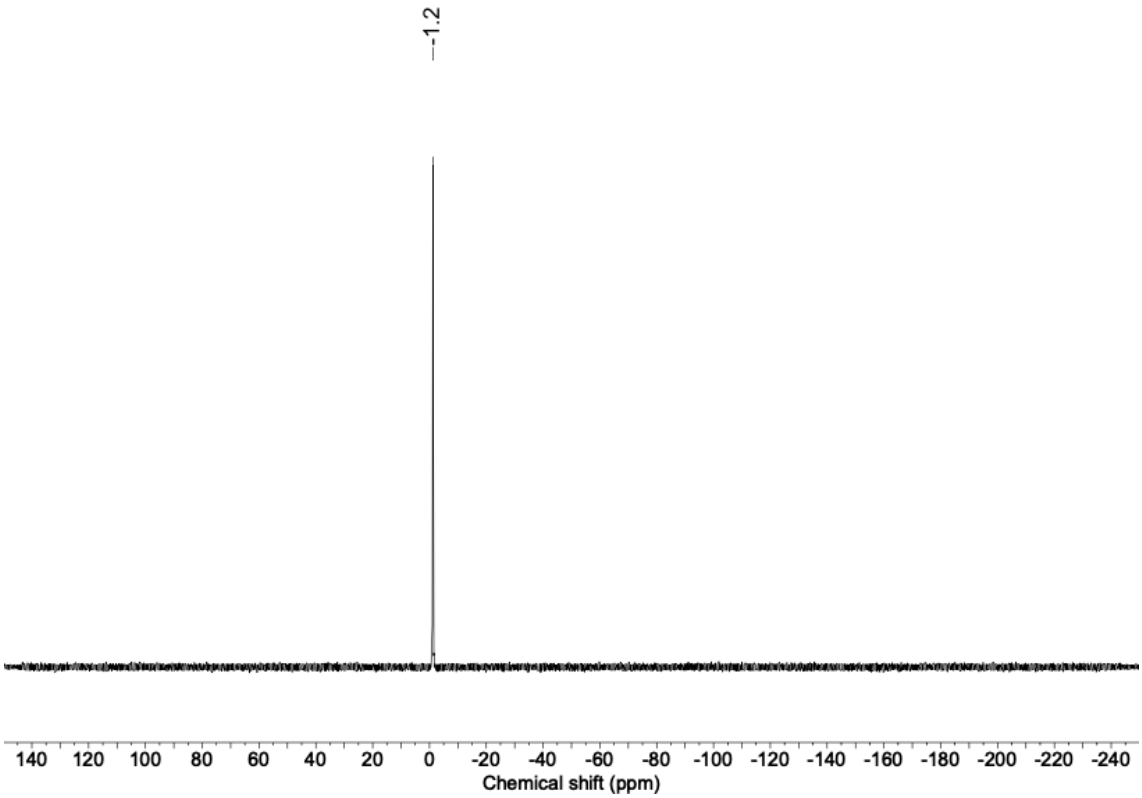

Figure S8. $^{31}P\{^{1}H\}$ (162 MHz, $(D_3C)_2SO$) NMR spectrum of [Au(*S*-2-thiocytosinate)(PMe_3)] (**2**).

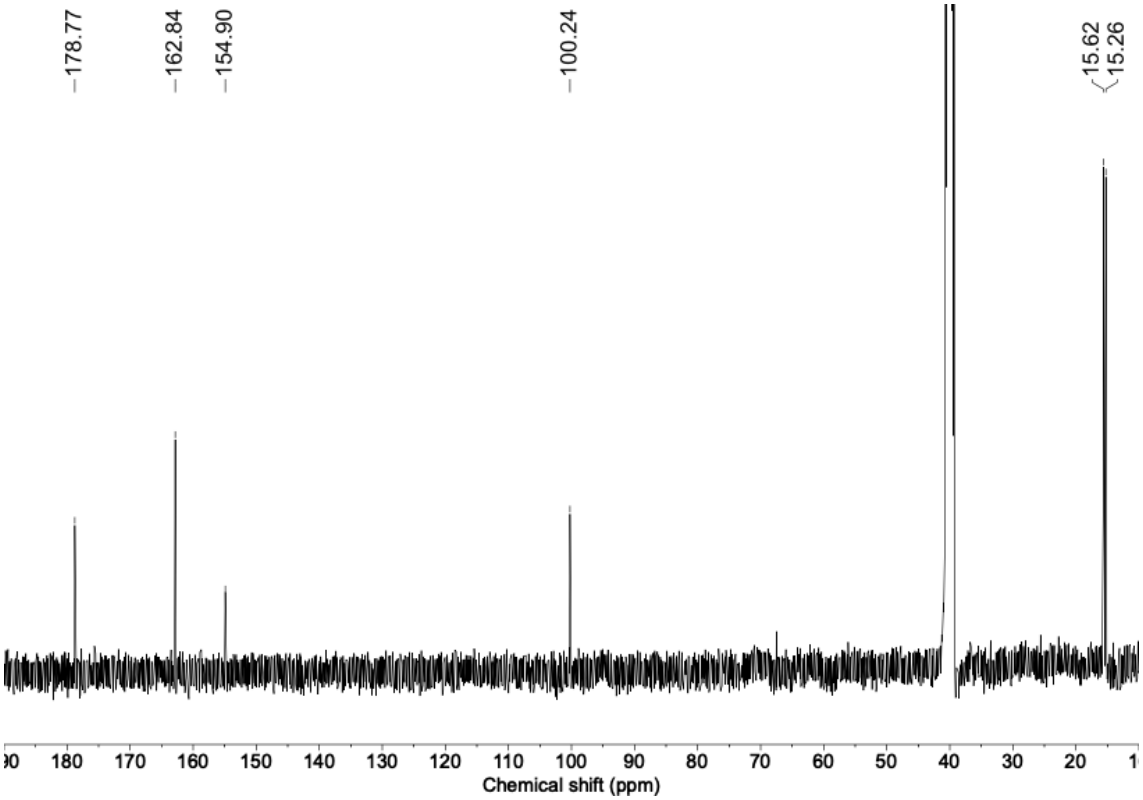

Figure S9. $^{13}C\{^{1}H\}$ (101 MHz, $(D_3C)_2SO$) NMR spectrum of [Au(*S*-2-thiocytosinate)(PMe_3)] (**2**).

3.4. ^{1}H, ^{19}F, $^{31}P\{^{1}H\}$ and $^{13}C\{^{1}H\}$ NMR spectra of [Au(*S*-2-thiocytosine)(PMe_3)](CF_3CO_2) (**3**).

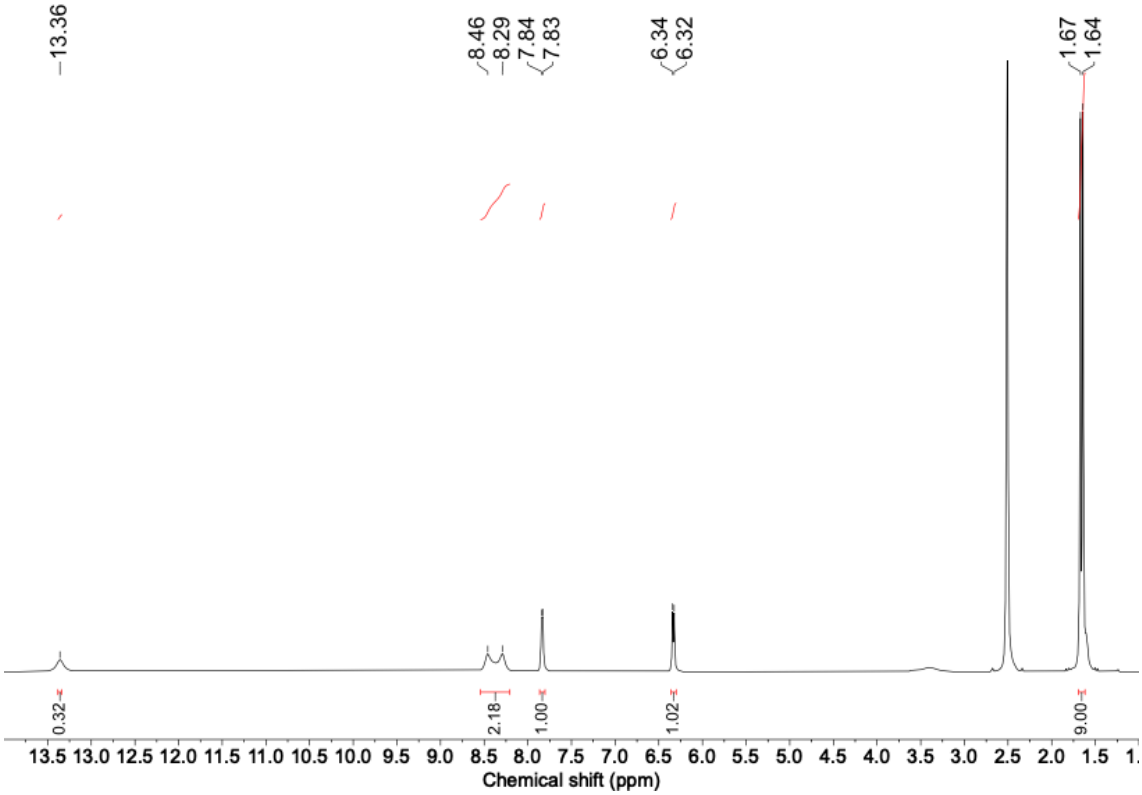

Figure S10. ^{1}H (400 MHz, $(D_3C)_2SO$) NMR spectrum of [Au(*S*-2-thiocytosine)(PMe_3)](CF_3CO_2) (**3**).

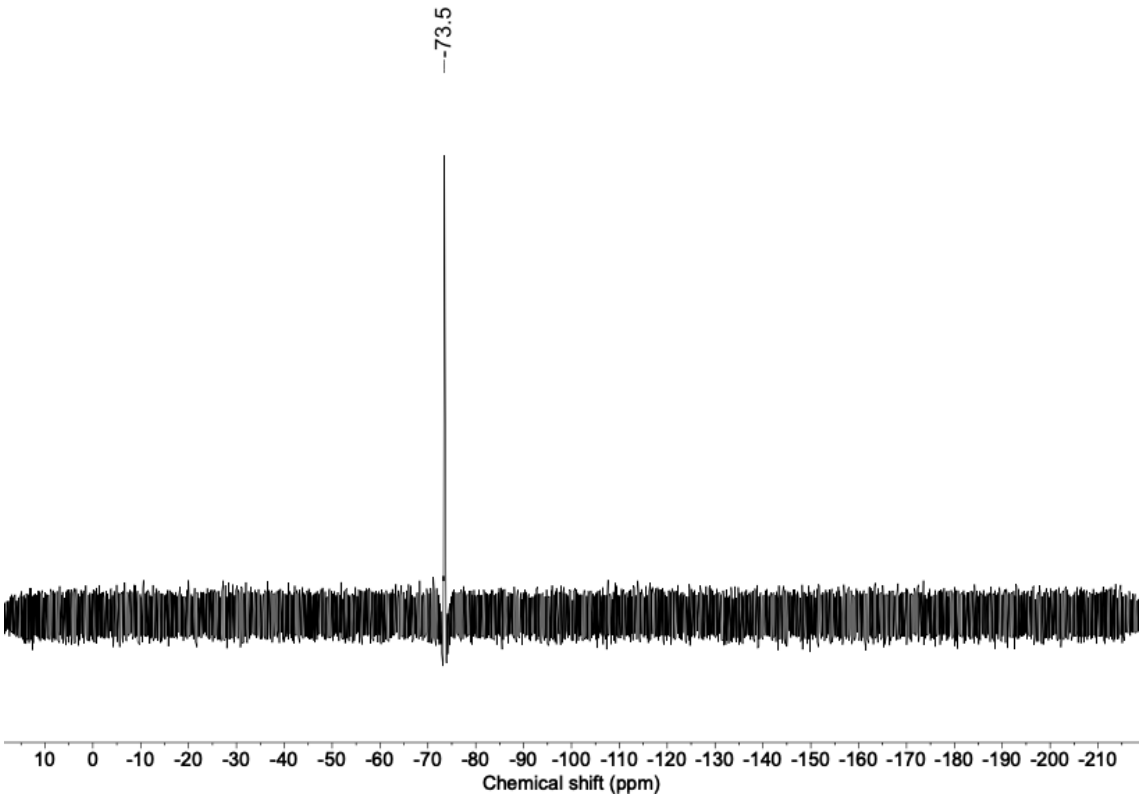

Figure S11. ^{19}F (282 MHz, $(D_3C)_2SO$) NMR spectrum of [Au(*S*-2-thiocytosine)(PMe_3)](CF_3CO_2) (**3**).

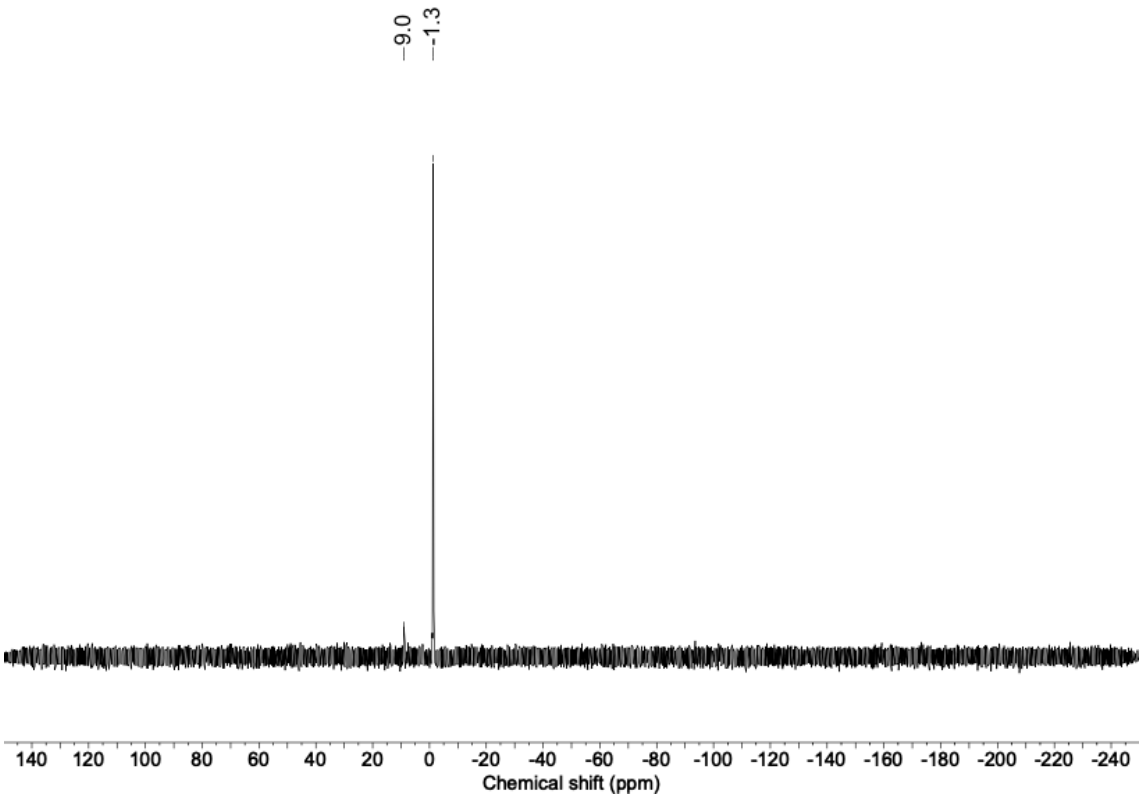

Figure S12. $^{31}P\{^{1}H\}$ (162 MHz, $(D_3C)_2SO$) NMR spectrum of [Au(*S*-2-thiocytosine)(PMe_3)](CF_3CO_2) (**3**). The minor peak at 9.0 ppm corresponds to $[Au(PMe_3)_2]^+$ cation.

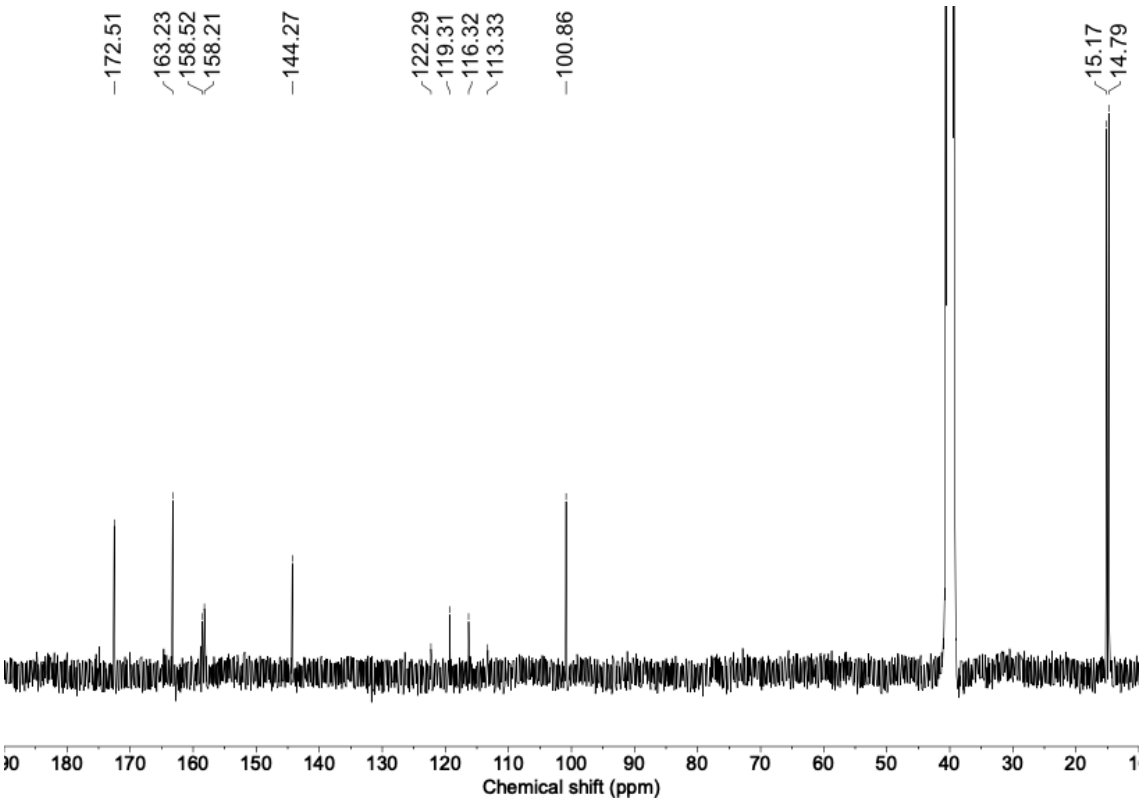

Figure S13. $^{13}C\{^{1}H\}$ (101 MHz, $(D_3C)_2SO$) NMR spectrum of [Au(*S*-2-thiocytosine)(PMe_3)](CF_3CO_2) (**3**).

3.5. ^{1}H, ^{19}F and $^{31}P\{^{1}H\}$ NMR spectra of [{Au(PMe_3)}$_2$(μ-*S,N*^{1}-2-thiocytosinate)](CF_3CO_2) (**4**).

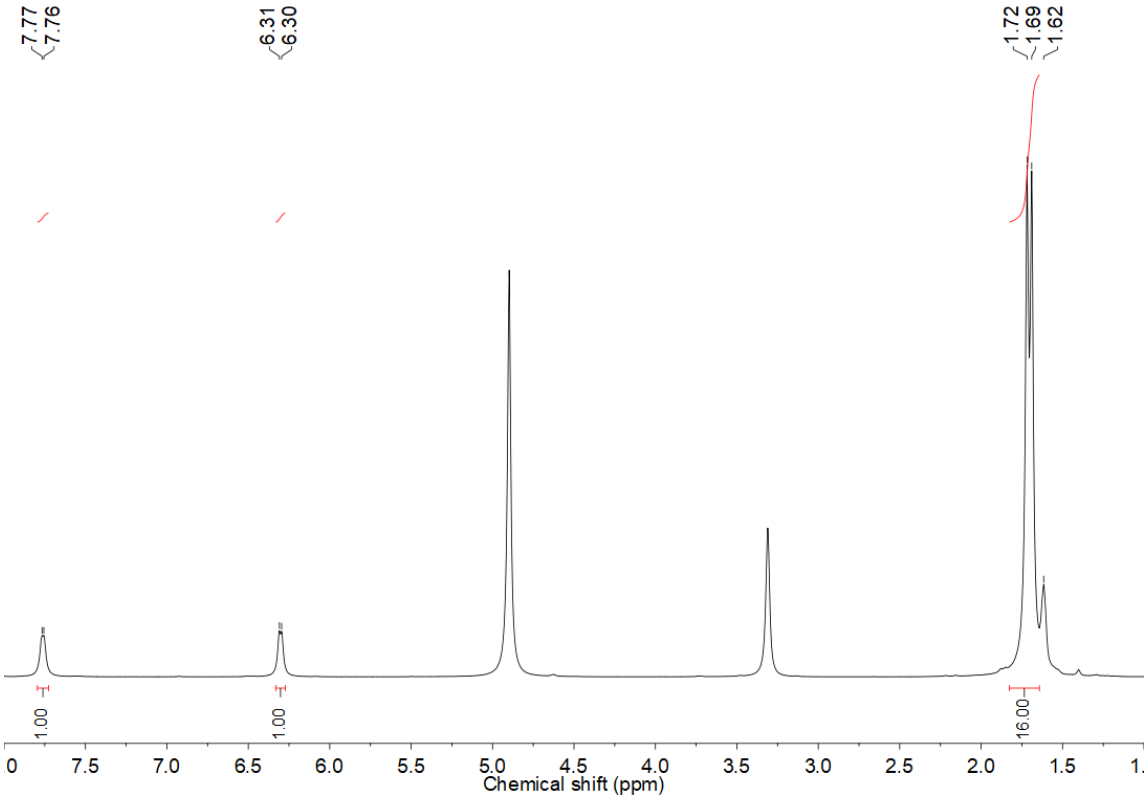

Figure S14. ^{1}H (400 MHz, CD_3OD) NMR spectrum of [{Au(PMe_3)}$_2$(μ-*S,N*^{1}-2-thiocytosinate)](CF_3CO_2) (**4**).

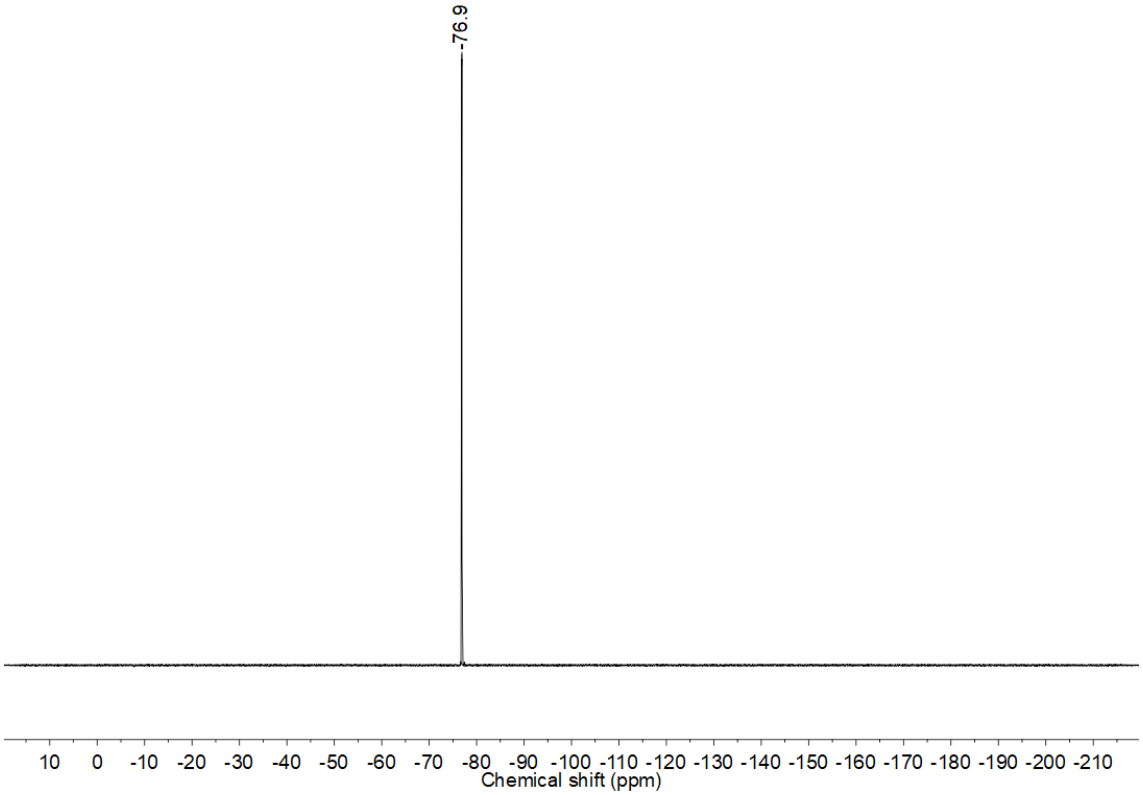

Figure S15. ^{19}F (376 MHz, CD_3OD) NMR spectrum of [{Au(PMe_3)}$_2$(μ-*S,N*^{1}-2-thiocytosinate)](CF_3CO_2) (**4**).

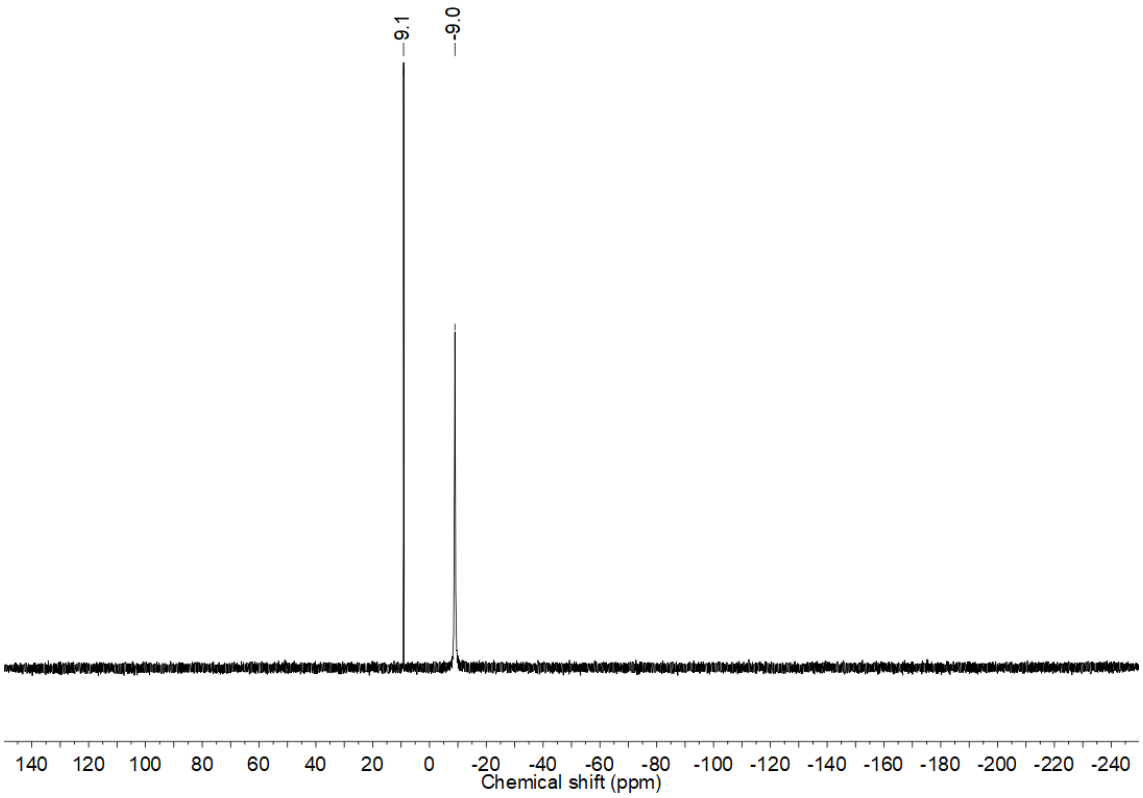

Figure S16. $^{31}P\{^{1}H\}$ (162 MHz, CD_3OD) NMR spectrum of [{Au(PMe_3)}$_2$(μ-*S,N*^{1}-2-thiocytosinate)](CF_3CO_2) (**4**). The peak at 9.1 ppm corresponds to $[Au(PMe_3)_2]^+$ cation.

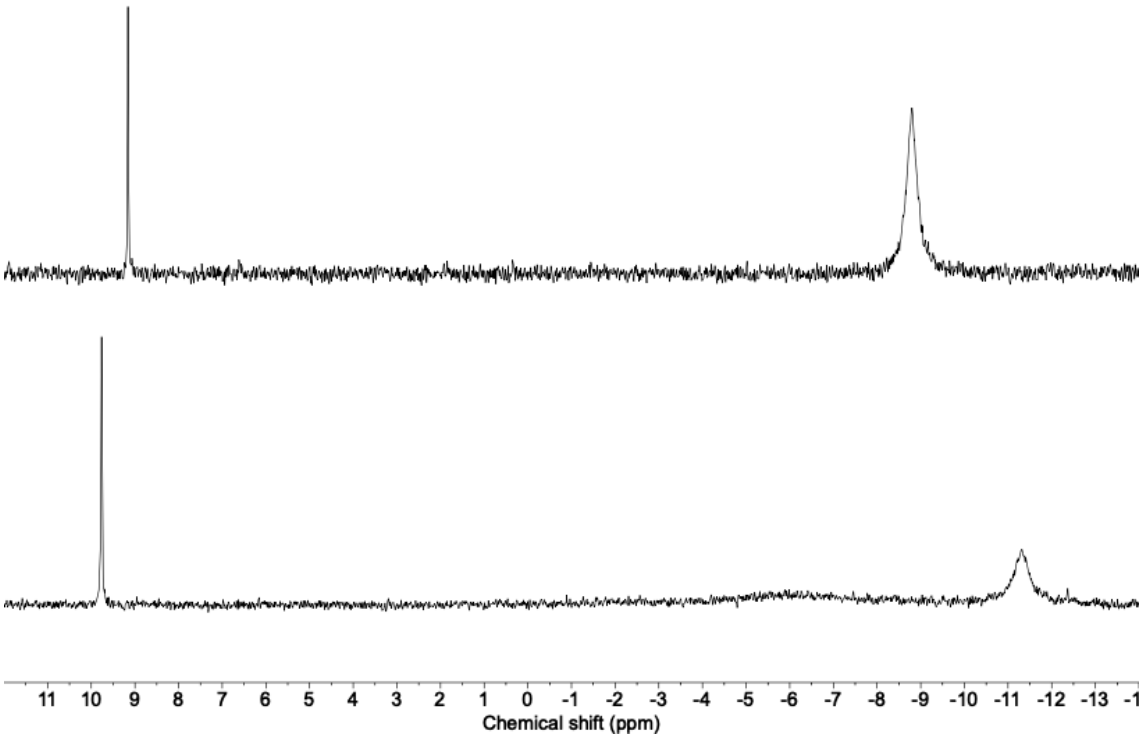

Figure S17. ^{1}H (400 MHz, CD_3OD) NMR spectra of [{Au(PMe_3)}$_2$(μ-*S,N*^{1}-2-thiocytosinate)](CF_3CO_2) (**4**) at room temperature (top) and at 200 K (bottom).

3.6. ESI-MS(+) spectra.

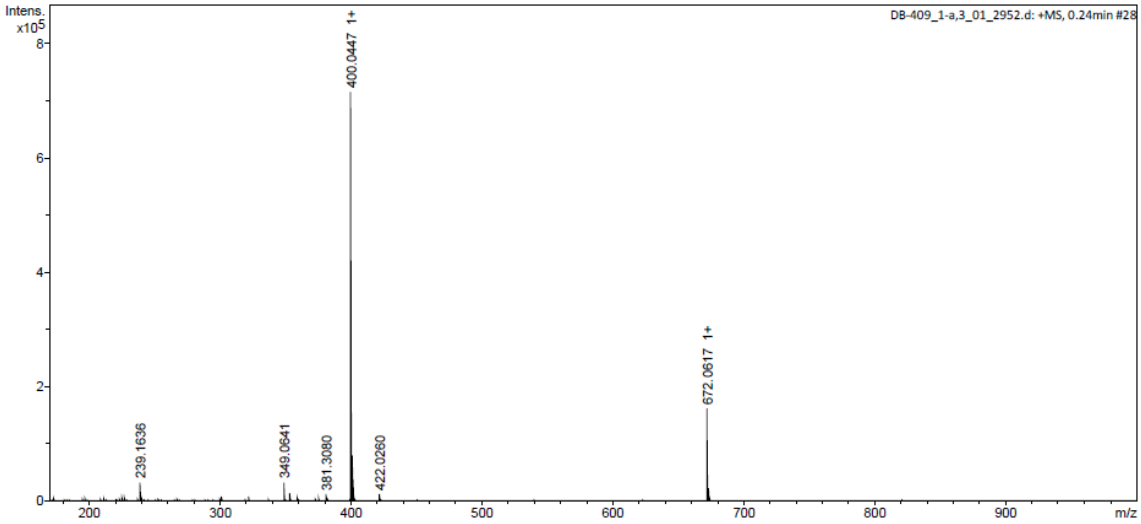

Figure S18. ESI-MS(+) spectrum of [Au(*S*-2-thiocytosinate)(PMe_3)] (**2**).

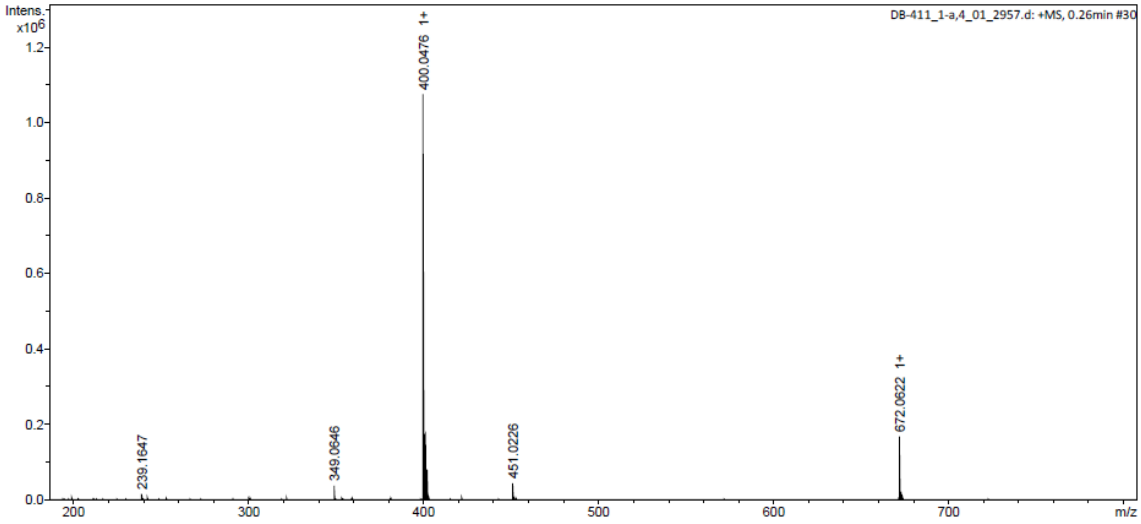

Figure S19. ESI-MS(+) spectrum of [Au(*S*-2-thiocytosine)(PMe_3)](CF_3CO_2) (**3**).

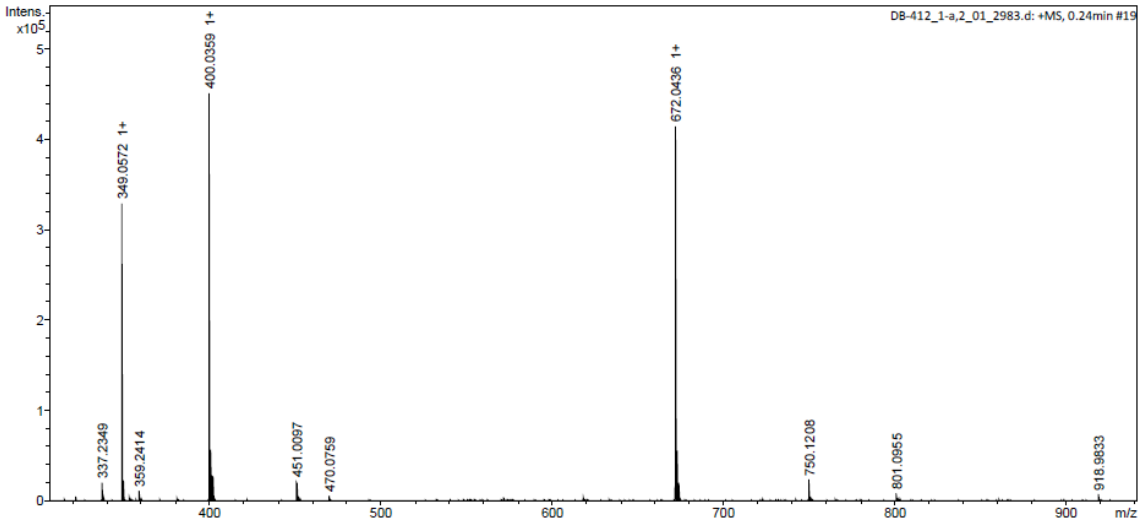

Figure S20. ESI-MS(+) spectrum of [{Au(PMe_3)}$_2$(μ-*S,N*^{1}-2-thiocytosinate)](CF_3CO_2) (**4**).

3.7. ESI-MS(-) spectra.

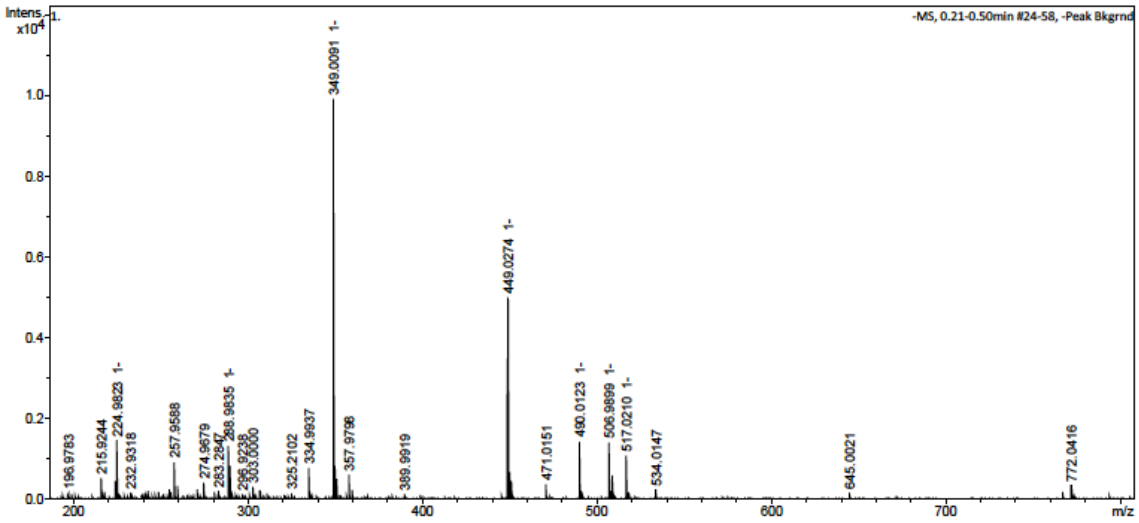

Figure S21. ESI-MS(-) spectrum of [Au(*S*-2-thiocytosinate)(PMe_3)] (**2**).

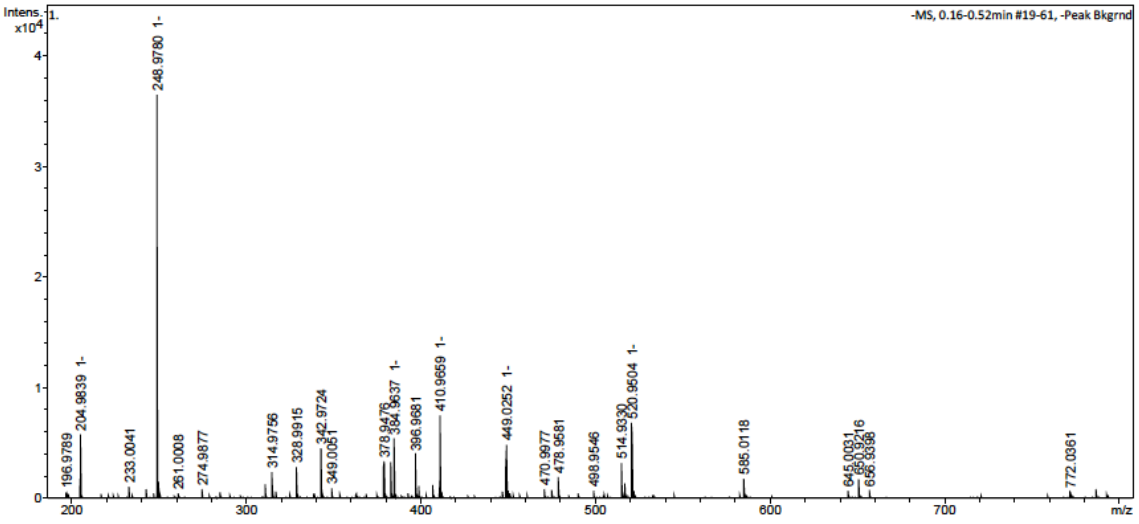

Figure S22. ESI-MS(-) spectrum of [Au(*S*-2-thiocytosine)(PMe_3)](CF_3CO_2) (**3**).

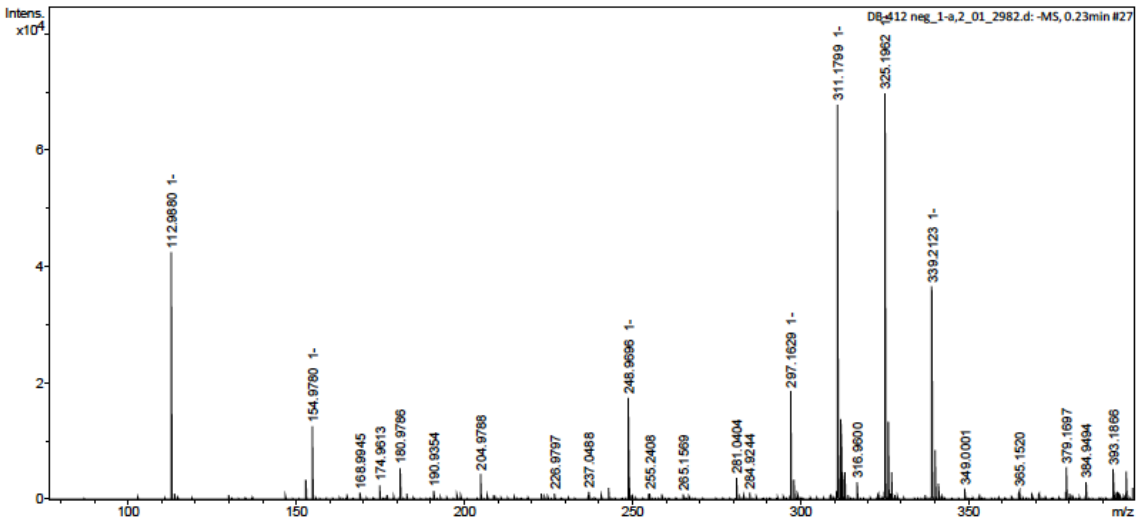

Figure S23. ESI-MS(-) spectrum of [{Au(PMe_3)}$_2$(μ-*S*,N^1-2-thiocytosinate)](CF_3CO_2) (**4**).

4. Structural characterization of complexes **2**-**4**·0.25H_2O.

Table S1. Data collection and structure refinement details for **2**-**4**·0.25H_2O.

Parameter	Value(s) (for **2**)	Value(s) (for **3**)	Value(s) (for **4**·0.25H_2O)
Empirical formula	$C_7H_{13}AuN_3PS$	$C_9H_{14}AuF_3N_3O_2PS$	$C_{12}H_{22}Au_2F_3N_3O_2P_2S·0.25H_2O$
Formula mass	399.20	513.23	789.76
Crystal habit	Colorless prism	Yellow plate	Colorless prism
Temperature	100.0 K	100.0 K	100.0 K
Wavelength	0.71073 Å	0.71073 Å	0.71073 Å
Crystal system	Orthorhombic	Orthorhombic	Monoclinic
Space group	*P* bca	*P* bca	*P* 2_1/c
Unit cell dimensions	*a* = 10.0240(6) Å α = 90º *b* = 11.6716(8) Å β = 90º *c* = 19.0849(12) Å γ = 90º	*a* = 21.823(2) Å α = 90º *b* = 12.7534(11) Å β = 90º *c* = 11.4368(10) Å γ = 90º	*a* = 20.087(2) Å α = 90º *b* = 17.9784(17) Å β = 93.051(4)º *c* = 12.3196(11) Å γ = 90º
Volume	2232.9(2) Å^3	3183.1(5) Å^3	4442.6(7) Å^3
Z	8	8	8
Density (calculated)	2.375 Mg m^{-3}	2.142 Mg m^{-3}	2.362 Mg·m^{-3}
Absorption coefficient	13.468 mm^{-1}	9.508 mm^{-1}	13.468 mm^{-1}
F(000)	1488.0	1935	2916.0
Crystal size	0.327 x 0.091 x 0.053 mm^3	0.300 x 0.125 x 0.018 mm^3	0.430 x 0.155 x 0.014 mm^3
ϑ range ($2\vartheta_{max}$/º)	3.426 – 27.884 (56)	3.035 – 26.729 (56)	2.791 – 27.961 (56)
Index ranges	-12 <= *h* <= 13 -15 <= *k* <= 15 -25 <= *l* <= 25	-27 <= *h* <= 27 -14 <= *k* <= 16 -14 <= *l* <= 14	-26 <= *h* <= 26 -23 <= *k* <= 23 -16 <= *l* <= 16
Total reflections	57956	63617	133062
Independent reflections	2656 [R_{int} = 0.0258]	3375 [R_{int} = 0.0933]	10624 [R_{int} = 0.1221]
Completeness to ϑ = 25.242º	99.4 %	99.8 %	99.8 %
Refinement method	Full-matrix least-squares on F^2	Full-matrix least-squares on F^2	Full-matrix least-squares on F^2
Data / Restrains / Parameters	2656 / 15 / 122	3375 / 30 / 184	10624 / 60 / 463
Goodness-of-fit on F^2	1.104	1.196	1.128
Final R indexes [$I > 2\sigma(I)$]	R_1 = 0.0173, wR_2 = 0.0464	R_1 = 0.0901, wR_2 =0.2180	R_1 = 0.0561, wR_2 = 0.1249
R indexes (all data)	R_1 = 0.0176, wR_2 = 0.0466	R_1 = 0.1190, wR_2 =0.2372	R_1 = 0.0875, wR_2 = 0.1424
Largest diff. peak and hole (e/Å^3)	1.584, -0.701	3.049, -6.444	2.399, -1.092

Table S2. Selected bond lengths (Å) and angles (°) for **2**.

Au(1)-S(1)	2.3222(7)
Au(1)-P(1)	2.2564(7)
S(1)-Au(1)-P(1)	177.14(3)

Table S3. Selected hydrogen bond lengths (Å) and angles (°) for **2**.

D-H···A	d(D-H)	d(H···A)	d(D···A)	θ(D-H···A)
N(3)-H(3A)···S(1)$^{\#1}$	0.88	2.820	3.651(3)	158.10
N(3)-H(3B)···N(1)$^{\#2}$	0.88	2.142	2.959(3)	154.14
C(3)-H(3)···S(1)$^{\#2}$	0.95	2.823	3.771(3)	175.73
C(2)-H(2)···N(2)$^{\#3}$	0.95	2.596	3.404(4)	143.09
C(5)-H(5C)···N(1)$^{\#4}$	0.98	2.646	3.620(4)	172.67
C(7)-H(7A)···N(2)$^{\#5}$	0.98	2.591	3.556(4)	168.29

Symmetry transformations used to generate equivalent atoms:
#1: -x + 3/2, y – 1/2, z; **#2**: -x + 1, y – 1/2, -z + 3/2; **#3**: x – 1/2, y, -z + 3/2; **#4**: -x + 1, -y + 1, -z + 1; **#5**: x +1/2, -y + 1/2, -z + 1.

Table S4. Selected bond lengths (Å) and angles (°) for **3**.

Au(1)-S(1)	2.332(6)
Au(1)-P(1)	2.245(7)
S(1)-Au(1)-P(1)	178.2(2)

Table S5. Selected bond lengths (Å) and angles (°) for **4**·0.25H_2O.

Au(1)-S(1)	2.331(3)
Au(1)-P(1)	2.251(3)
Au(2)-N(1)	2.091(11)
Au(2)-P(2)	2.235(4)
Au(2)···Au(1)$^{\#1}$	3.0371(7)
Au(3)-S(2)	2.324(3)
Au(3)-P(3)	2.254(3)
Au(4)-N(4)	2.091(10)
Au(4)-P(4)	2.238(3)
Au(4)···Au(3)$^{\#1}$	3.1316(7)
P(1)-Au(1)-S(1)	177.19(12)
P(2)-Au(2)-N(1)	179.2(3)
P(2)-Au(2)···Au(1)$^{\#1}$	98.35(10)
N(1)-Au(2)···Au(1)$^{\#1}$	81.9(3)
S(1)-Au(1)···Au(2)$^{\#2}$	80.10(8)
P(1)-Au(1)···Au(2)$^{\#2}$	102.67(9)
P(3)-Au(3)-S(2)	173.42(12)
P(4)-Au(4)-N(4)	173.3(3)
P(4)-Au(4)···Au(3)$^{\#1}$	97.35(9)
N(4)-Au(4)···Au(3)$^{\#1}$	83.8(3)
S(2)-Au(3)···Au(4)$^{\#2}$	81.76(8)
P(3)-Au(3)···Au(4)$^{\#2}$	104.68(10)

Symmetry transformations used to generate equivalent atoms:
#1: x, -y + 1/2, z – 1/2; **#2**: x, -y + 1/2, z + 1/2.

Table S6. Selected hydrogen bond lengths (Å) and angles (°) for **4**·0.25H_2O.

D-H···A	d(D-H)	d(H···A)	d(D···A)	θ(D-H···A)
N(3)-H(3A)···O(4)$^{\#1}$	0.88	2.028	2.905(14)	173.43
N(3)-H(3B)···O(1)$^{\#2}$	0.88	1.973	2.816(16)	159.66
N(6)-H(6D)···O(2)$^{\#3}$	0.88	2.067	2.922(16)	163.41
N(6)-H(6E)···O(3)$^{\#4}$	0.88	1.987	2.855(16)	168.94
O(5)-H(5E)···O(2)$^{\#5}$	0.87	1.867	2.689	157.09

Symmetry transformations used to generate equivalent atoms:
#1: -x, -y, -z + 2; **#2**: -x, y – 1/2, -z + 3/2; **#3**: x + 1, y, z; **#4**: x + 1, -y + 1/2, z – 1/2; **#5**: x, -y + 1/2, z – 1/2.

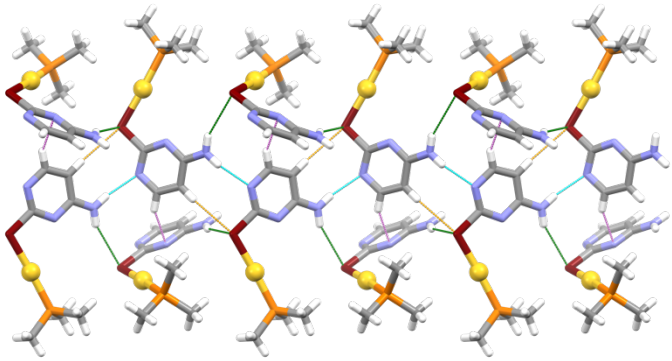

Figure S24. Supramolecular expansion of **2** through ^{4}CN-H···^{1}N (blue dashes), ^{4}CN-H···S (green dashes), ^{5}C-H···S (orange dashes) and ^{6}C-H···^{3}N (violet dashes) hydrogen bonds. Colour code: C, grey; H, white; Au, yellow; N, blue; P, orange; S, brown.

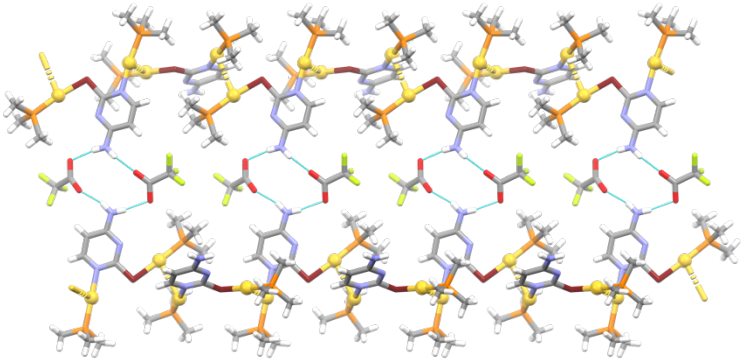

Figure S25. Supramolecular expansion of **4**·0.25H_2O through ^{4}CN-H···O (blue dashes) hydrogen bonds (water molecules have been omitted for clarity). Colour code: C, grey; H, white; Au, yellow; F, green; N, blue; O, red; P, orange; S, brown.

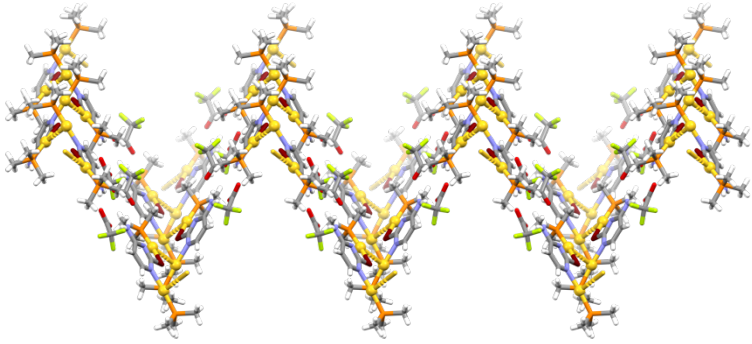

Figure S26. Supramolecular expansion of **4**·0.25H_2O into a complex 2-D folded sheet-like pattern (water molecules have been omitted for clarity). Colour code: C, grey; H, white; Au, yellow; F, green; N, blue; O, red; P, orange; S, brown.

5. Optical properties (solid state).

5.1. DRUV-Vis spectra (KBr mulls).

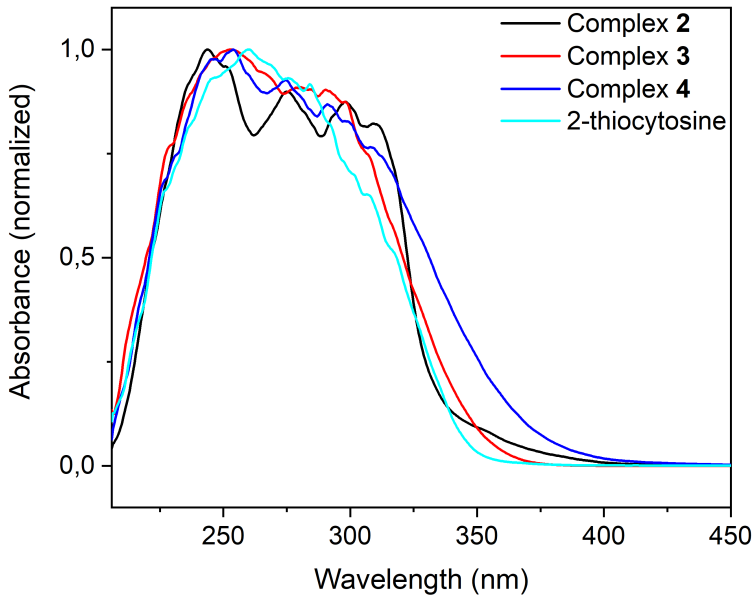

Figure S27. Superimposition of the absorption spectra of complexes [Au(*S*-2-thiocytosinate)(PMe_3)] (**2**, black line), [Au(*S*-2-thiocytosine)(PMe_3)](CF_3CO_2) (**3**, red line), [{Au(PMe_3)}$_2$(μ-*S*,N^1-2-thiocytosinate)](CF_3CO_2) (**4**, blue line) and free 2-thiocytosine (cyan line), in anhydrous KBr mulls.

5.2. Lifetime decay parameters of complexes **2**-**4**.

Single Photon Counting data were fitted to the multiexponential decay function (**Equation S1**):

$$f(i) = A + \sum_n B_n \cdot \exp\left(-\frac{i}{T_n}\right) \qquad \textbf{Equation S1}$$

where A, B_n and T_n are free fitting parameters, and n is a variable integer between 1 and 4.

The emission lifetimes were calculated according to **Equation S2**:

$$\tau(s) = \sum_n T_n(s) \cdot \frac{B_n}{\sum_n B_n} \qquad \textbf{Equation S2}$$

Lifetime decay parameters for complex **2** at 298 K (*n* = 3):

λ_{exn} = 370 nm

λ_{ems} = 520 nm

n	T_n (channels)	T_n (s)	σ_n (s)	B_n	Rel. Ampl. (%)	σ_n
1	207.7243	3.647285E-07	9.048968E-09	2726.721	31.62	11.49801
2	975.988	1.713669E-06	2.04653E-08	1164.665	63.46	4.030958
3	39.13415	6.871291E-08	1.444444E-09	2251.217	4.92	23.42017

A = 557.1447; χ^2 = 1.070662 (3357 degrees of freedom); τ = 512 ns.

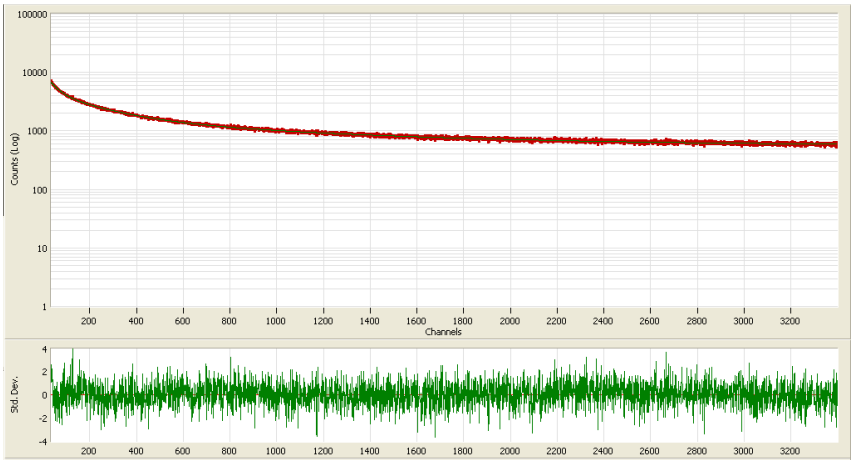

Lifetime decay parameters for complex **3** at 77 K (*n* = 3):

λ_{exn} = 370 nm

λ_{ems} = 458 nm

n	T_n (channels)	T_n (s)	σ_n (s)	B_n	Rel. Ampl. (%)	σ_n
1	254.6852	4.471839E-07	3.217615E-08	396.5511	15.79	5.136616
2	1027.088	1.803392E-06	2.403083E-08	507.1555	81.43	2.282107
3	27.3435	4.801054E-08	1.891899E-09	651.0259	2.78	12.48437

A = 181.5983; χ^2 = 1.012728 (3925 degrees of freedom); τ = 722 ns.

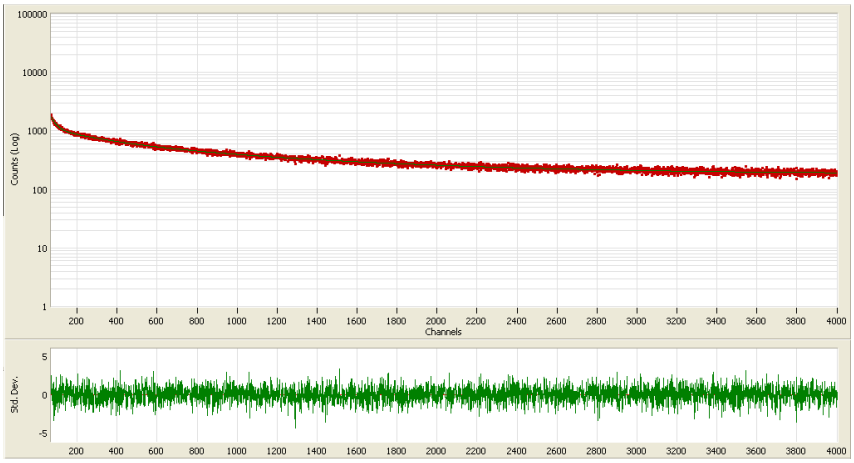

Lifetime decay parameters for complex **4** at 298 K (*n* = 3):

λ_{exn} = 390 nm

λ_{ems} = 520 nm

n	T_n (channels)	T_n (s)	σ_n (s)	B_n	Rel. Ampl. (%)	σ_n
1	1.511483	5.307814E-09	6.604497E-09	77.54923	0.25	17.79173
2	74.53543	2.617431E-07	2.108335E-08	135.8336	21.94	3.769272
3	442.0701	1.5524E-06	5.467881E-08	81.22614	77.81	1.403569

A = 117.7655; χ^2 = 0.9753762 (3561 degrees of freedom); τ = 550 ns.

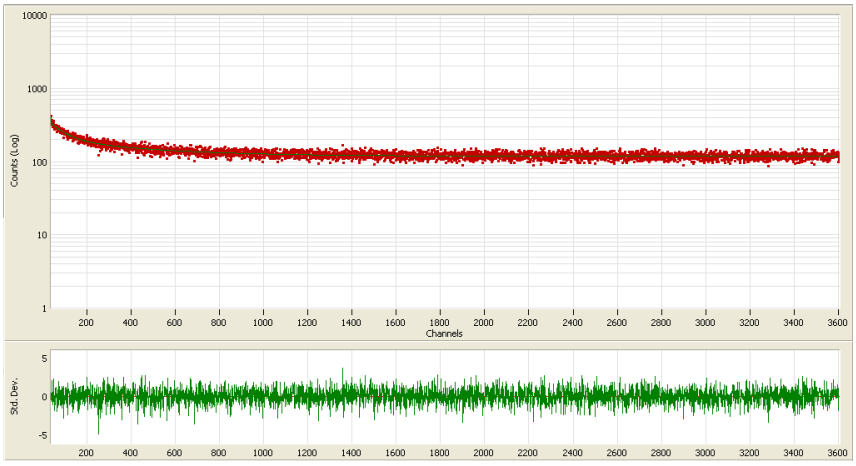

6. Computational studies.

Table S7. Population analysis of model **2a**.

Orbital	Contribution (%)		
	Trimethylphosphine	2-thiocytosinate	Au^{I}
48 (LUMO+4)	3	88	9
47 (LUMO+3)	10	68	23
46 (LUMO+2)	24	1	75
45 (LUMO+1)	7	5	88
44 (LUMO)	14	35	51
43 (HOMO)	1	91	8
42 (HOMO-1)	1	77	23
41 (HOMO-2)	0	98	2

Table S8. Most relevant TD-DFT singlet-to-singlet and singlet-to-triplet transitions of model **2a**.

	Transition	Wavelength (nm)	Oscillator strength	Contributions (%)			
B	$S_0 \rightarrow S_1$	303.33	0.1335	HOMO	→	LUMO	(96)
C	$S_0 \rightarrow S_5$	263.00	0.0432	HOMO	→	LUMO+3	(83)
D	$S_0 \rightarrow S_8$	237.68	0.0807	HOMO-1	→	LUMO+1	(16)
				HOMO-1	→	LUMO+2	(36)
				HOMO-1	→	LUMO+4	(18)
E	$S_0 \rightarrow S_9$	236.93	0.1447	HOMO-1	→	LUMO+2	(16)
				HOMO-1	→	LUMO+4	(20)
				HOMO	→	LUMO+4	(32)
F	$S_0 \rightarrow S_{12}$	228.92	0.0648	HOMO-2	→	LUMO	(82)
A	$S_0 \rightarrow T_1$	364.03	Spin-forbidden	HOMO	→	LUMO	(59)
				HOMO	→	LUMO+4	(20)

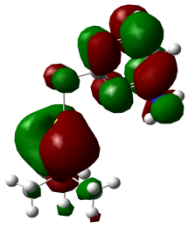

MO 47 (LUMO+3)

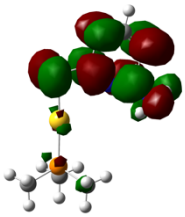

MO 48 (LUMO+4)

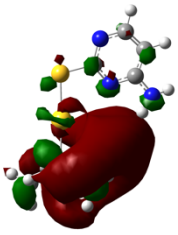

MO 45 (LUMO+1)

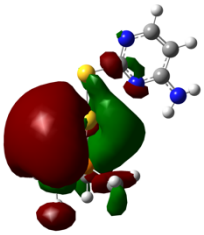

MO 46 (LUMO+2)

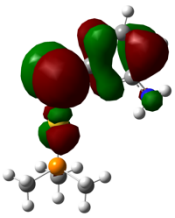

MO 43 (HOMO)

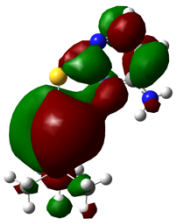

MO 44 (LUMO)

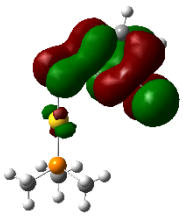

MO 41 (HOMO-2)

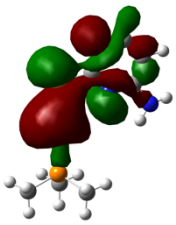

MO 42 (HOMO-1)

Figure S28. Orbitals involved in the most important transitions for model **2a**.

Table S9. Population analysis of model **4a**.

Orbital	Contribution (%)					
	$[Au(PMe_3)]^{\#1}$	2-TC$^{\#1}$	$[Au(PMe_3)]^{\#2}$	$[Au(PMe_3)]^{\#3}$	2-TC$^{\#2}$	[Au(PMe3)]$^{\#4}$
134 (LUMO+3)	6	12	3	14	59	7
132 (LUMO+1)	11	55	11	9	14	0
131 (LUMO)	3	78	10	5	4	0
130 (HOMO)	0	13	5	13	60	9
129 (HOMO-1)	1	27	9	16	41	6
128 (HOMO-2)	2	54	18	8	11	6
124 (HOMO-6)	7	3	29	11	24	26
123 (HOMO-7)	8	88	2	0	1	0

Key for the interpretation of the table:

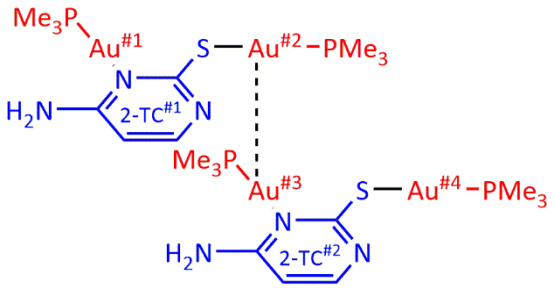

Table S10. Most relevant TD-DFT singlet-to-singlet and singlet-to-triplet transitions of model **4a**.

	Transition	Wavelength (nm)	Oscillator strength	Contributions (%)			
B	$S_0 \rightarrow S_1$	300.08	0.0398	HOMO-1	→	LUMO	(43)
				HOMO	→	LUMO	(43)
C	$S_0 \rightarrow S_3$	292.26	0.1287	HOMO-1	→	LUMO+1	(64)
D	$S_0 \rightarrow S_5$	282.46	0.1151	HOMO-1	→	LUMO	(16)
				HOMO-1	→	LUMO+2	(44)
				HOMO	→	LUMO	(18)
E	$S_0 \rightarrow S_{51}$	215.23	0.1269	HOMO-6	→	LUMO+3	(17)
F	$S_0 \rightarrow S_{55}$	212.67	0.1553	HOMO-7	→	LUMO+1	(16)
A	$S_0 \rightarrow T_1$	360.51	Spin-forbidden	HOMO-2	→	LUMO	(16)
				HOMO-1	→	LUMO	(17)

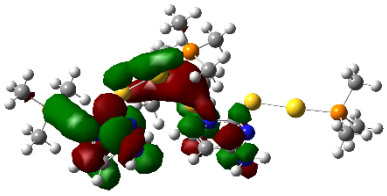

MO 132 (LUMO+1)

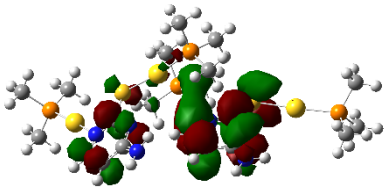

MO 134 (LUMO+3)

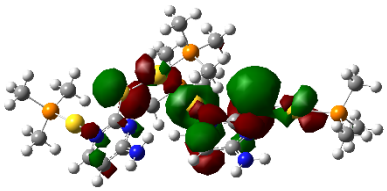

MO 130 (HOMO)

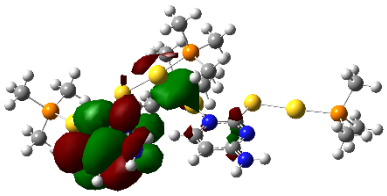

MO 131 (LUMO)

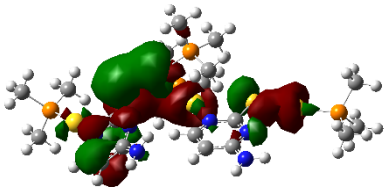

MO 128 (HOMO-2)

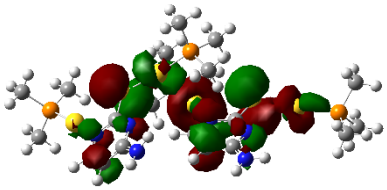

MO 129 (HOMO-1)

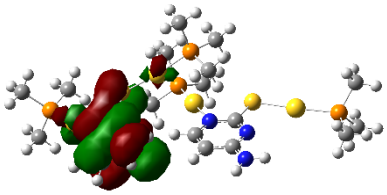

MO 123 (HOMO-7)

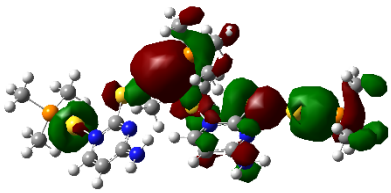

MO 124 (HOMO-6)

Figure S29. Orbitals involved in the most important transitions for model **4a**.

Table S11. Population analysis of model **4b**.

Orbital	Contribution (%)		
	Au^{I}	2-thiocytosinate	
		S	2-aminopyrimidine
127 (LUMO+6)	10	12	79
126 (LUMO+5)	7	4	89
125 (LUMO+4)	6	5	89
124 (LUMO+3)	5	9	86
123 (LUMO+2)	1	3	96
122 (LUMO+1)	3	2	95
121 (LUMO)	21	2	77
120 (HOMO)	68	24	8
119 (HOMO-1)	18	60	23
118 (HOMO-2)	64	28	8

Table S12. First TD-DFT singlet-to-singlet transitions of model **4b**.

Transition	Wavelength (nm)	Oscillator strength	Contributions (%)			
$S_0 \rightarrow S_1$	375.24	0.0229	HOMO	→	LUMO	(96)
$S_0 \rightarrow S_3$	354.45	0.0017	HOMO	→	LUMO+2	(90)
$S_0 \rightarrow S_4$	347.38	0.0046	HOMO-1	→	LUMO	(93)
$S_0 \rightarrow S_5$	345.54	0.0014	HOMO-2	→	LUMO	(29)
			HOMO	→	LUMO+3	(52)
$S_0 \rightarrow S_8$	332.11	0.0045	HOMO-2	→	LUMO+1	(27)
			HOMO-1	→	LUMO+2	(22)
			HOMO	→	LUMO+5	(29)
$S_0 \rightarrow S_{10}$	328.66	0.0098	HOMO-1	→	LUMO+2	(44)
			HOMO	→	LUMO+5	(35)

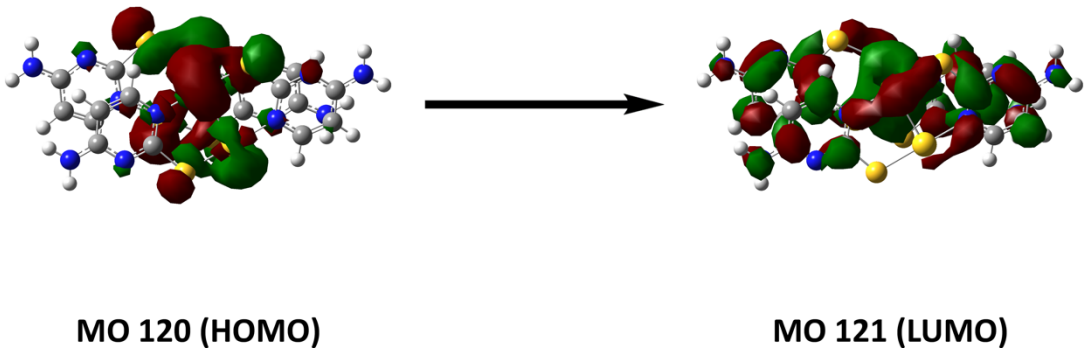

Figure S30. Orbitals involved in the $S_0 \rightarrow S_1$transition of model **4b**.

Table S13. Population analysis of model **4c**.

Orbital	Contribution (%)		
	Au^{I}	2-thiocytosinate	
		S	2-aminopyrimidine
125 (LUMO+4)	3	4	93
124 (LUMO+3)	3	14	83
123 (LUMO+2)	3	14	83
122 (LUMO+1)	27	1	72
121 (LUMO)	39	8	53
120 (HOMO)	66	25	9
119 (HOMO-1)	23	49	28
118 (HOMO-2)	23	49	28

Table S14. First TD-DFT singlet-to-singlet transitions of model **4c**.

Transition	Wavelength (nm)	Oscillator strength	Contributions (%)			
$S_0 \rightarrow S_1$	376.66	0.0161	HOMO	→	LUMO	(97)
$S_0 \rightarrow S_3$	335.20	0.0336	HOMO-2	→	LUMO	(55)
			HOMO-1	→	LUMO	(29)
$S_0 \rightarrow S_4$	335.20	0.0336	HOMO-2	→	LUMO	(29)
			HOMO-1	→	LUMO	(55)
$S_0 \rightarrow S_5$	325.48	0.0065	HOMO-1	→	LUMO+1	(20)
			HOMO	→	LUMO+2	(70)
$S_0 \rightarrow S_6$	325.48	0.0065	HOMO-2	→	LUMO+1	(20)
			HOMO	→	LUMO+3	(70)
$S_0 \rightarrow S_8$	318.51	0.0013	HOMO-1	→	LUMO+1	(57)
			HOMO	→	LUMO+2	(25)
$S_0 \rightarrow S_9$	318.50	0.0013	HOMO-2	→	LUMO+1	(57)
			HOMO	→	LUMO+3	(27)
$S_0 \rightarrow S_{10}$	313.13	0.0060	HOMO	→	LUMO+4	(82)

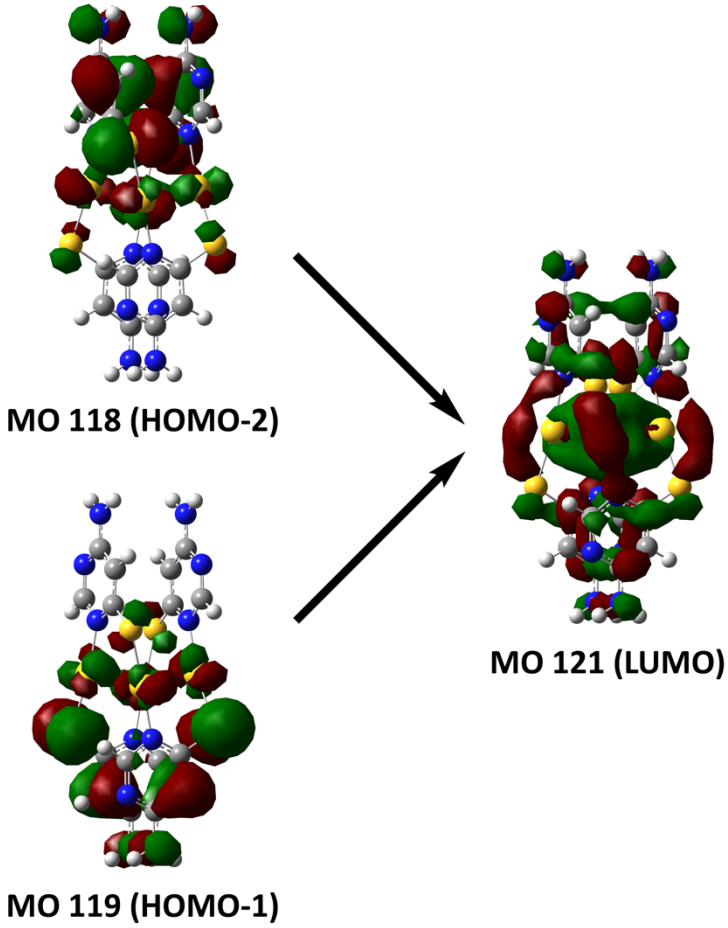

Figure S31. Orbitals involved in the $S_0 \longrightarrow S_3$ and $S_0 \longrightarrow S_4$ transitions of model **4c**.

7. Optical properties (solution) of complex **4**.

7.1. UV-Vis spectra.

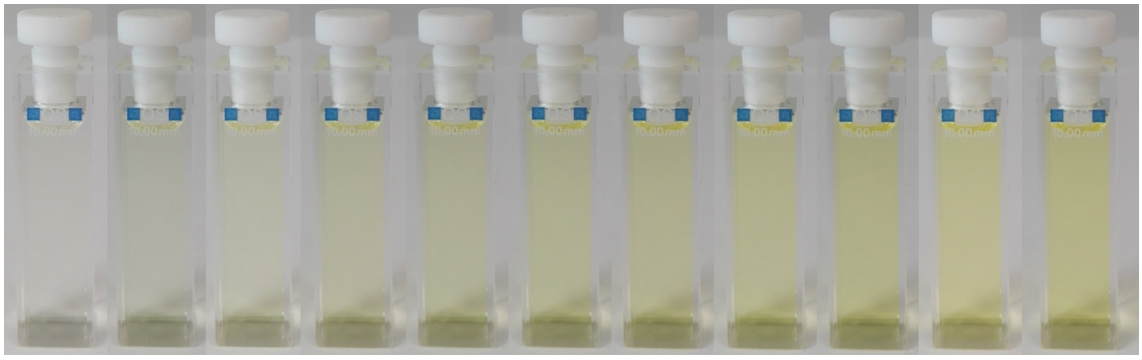

Figure S32. Photographs (taken every minute) of a diluted aqueous solution of complex **4**.

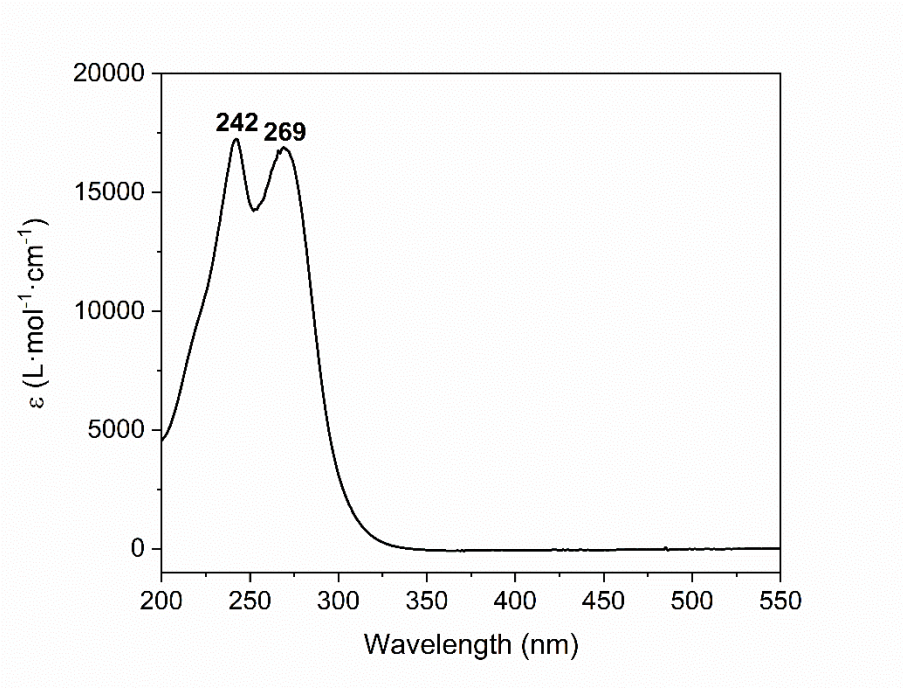

Figure S33. UV-Vis spectrum of 2-thiocytosine in aqueous solution.

7.2. Photoluminescence spectra.

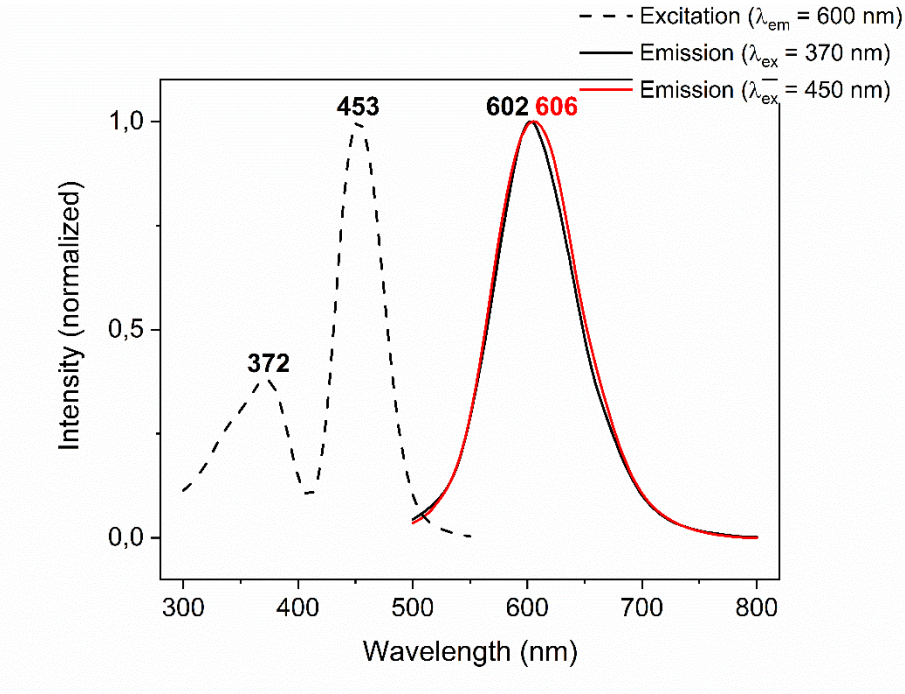

Figure S34. Luminescence spectra of an aged aqueous solution of complex **4** (0.5 mM), where the emission energy is shown to be apparently irrespective of the excitation wavelength.

7.3. Lifetime decay parameters.

Lifetime decay parameters for complex **4** (0.5 mM in distilled water, *n* = 3):

λ_{exn} = 450 nm

λ_{ems} = 600 nm

n	T_n (channels)	T_n (s)	σ_n (s)	B_n	Rel. Ampl. (%)	σ_n
1	95.75435	1.681284E-7	3.910289E-9	2505.959	45.52	11.96481
2	399.3895	7.012601E-7	7.399175E-9	506.6776	38.39	2.681014
3	20.31042	3.566165E-8	4.763819E-10	4175.303	16.09	29.91898

A = 108.0494; χ^2 = 1.050787 (3933 degrees of freedom); τ = 129 ns.

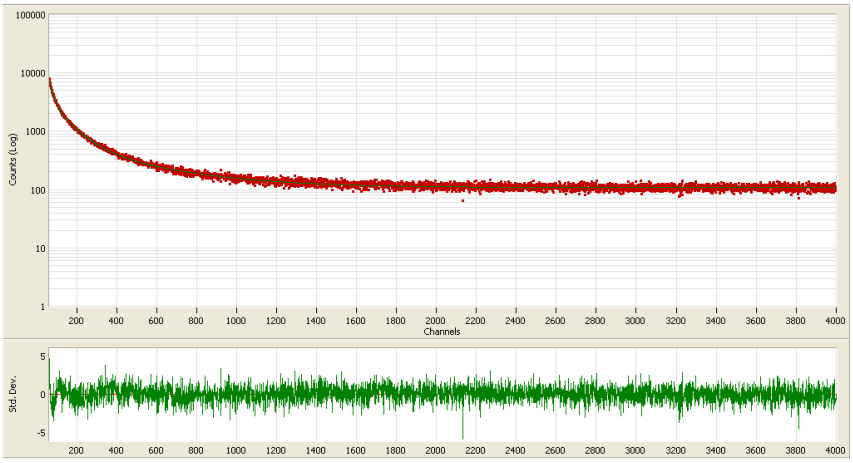

8. NMR kinetic studies of complex **4** (in D_2O).

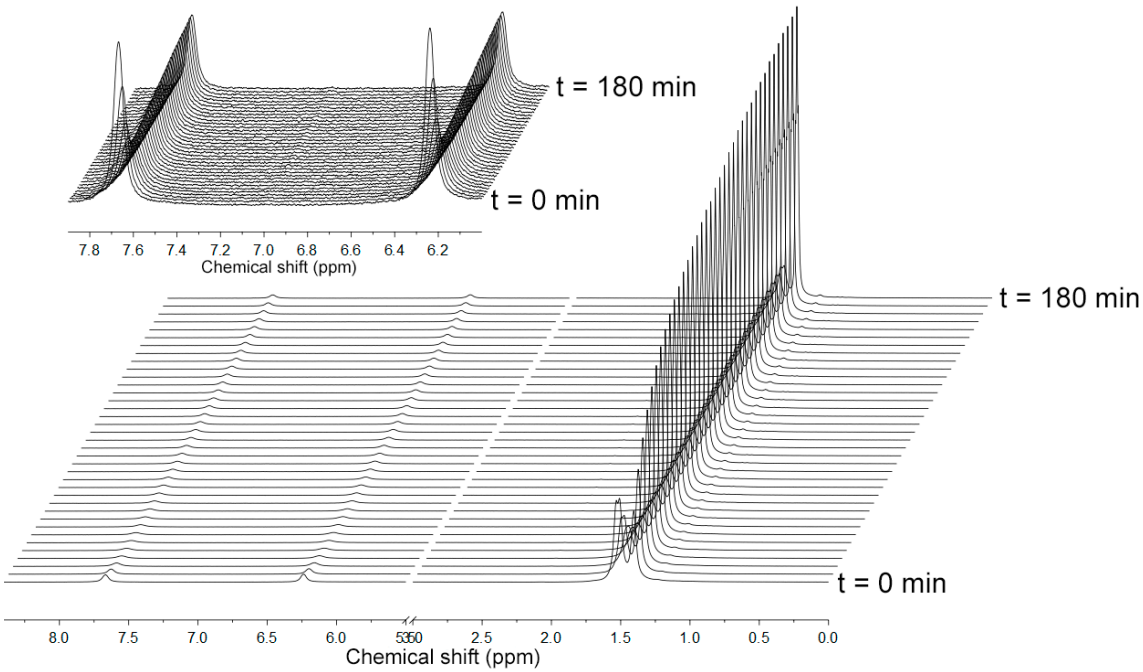

Figure S35. ^{1}H (400 MHz, D_2O) NMR spectra stacking of complex **4** along time (total dwell time between spectra of 300 s (5 min)). Inset: zoom of 2-thiocytosine resonances' region.

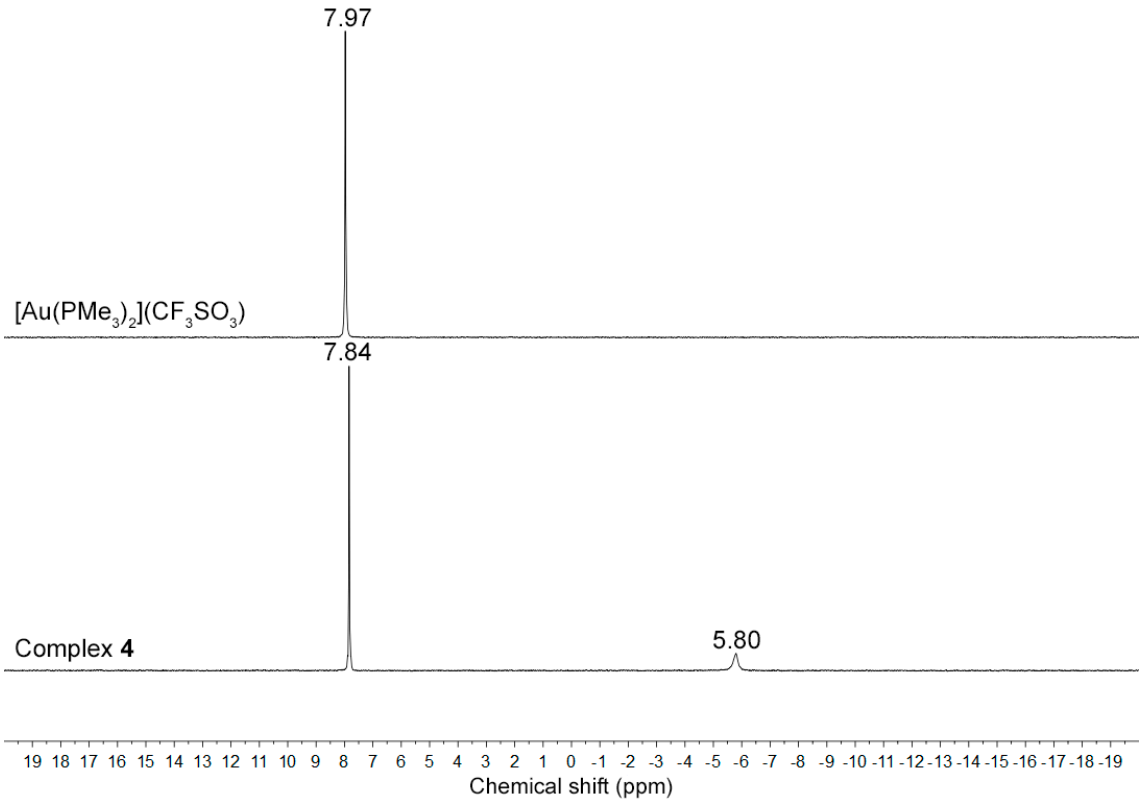

Figure S36. $^{31}P\{^{1}H\}$ (162 MHz, D_2O) NMR spectra of (top) $[Au(PMe_3)_2](CF_3SO_3)$ and (bottom) complex **4** after 3 h in solution.

9. Atomic coordinates of computational optimizations (xyz format).

Table S15. Cartesian coordinates of the optimized structure of model **2a** (DFT-D3/PBE).

Au	0.68072300	-0.57251500	-0.01558600
S	-1.24504200	-1.88735400	-0.03150700
P	2.63110300	0.62508700	0.02346900
N	-3.73827300	-1.06936000	0.05404600
N	-2.10176600	0.65279500	-0.04654100
N	-2.65061300	2.87679600	-0.00856900
H	-1.69809700	3.01585000	-0.32136600
H	-3.31576300	3.57137300	-0.31884500
C	-2.48139200	-0.62953500	-0.00316200
C	-4.67897800	-0.13084400	0.08080800
H	-5.71372100	-0.48913600	0.12619000
C	-4.41563200	1.22388100	0.05489300
H	-5.21124900	1.97016400	0.08734800
C	-3.05876800	1.57654800	-0.01307800
C	4.14776000	-0.37504200	0.30271600
H	5.04421200	0.26224600	0.31410500
H	4.23215900	-1.12274300	-0.49733300
H	4.05320800	-0.90230100	1.26153200
C	2.71163000	1.91260000	1.33432100
H	2.60171900	1.42851200	2.31409300
H	1.87377400	2.60969900	1.19875300
H	3.66446800	2.46058400	1.29284500
C	3.00524400	1.55713100	-1.51767000
H	3.94780700	2.11650100	-1.42398400
H	2.17926200	2.25165100	-1.72228400
H	3.07462400	0.84757700	-2.35322000

Table S16. Cartesian coordinates of the optimized structure of model **4a** (DFT-D3/PBE).

Au	0.42442125	-0.96819452	0.24446108
Au	5.88007249	-0.57746816	0.52212439
S	3.56423695	-0.83862538	0.20490270
P	-0.73387664	-2.89334281	-0.15276924
P	8.16473393	-0.51558670	0.80712602
N	1.53502889	0.73620799	0.74892577
N	3.66634085	1.67154789	1.13945898
N	3.91808459	3.78109562	1.95162898
H	4.91141863	3.59406002	1.97655750
H	3.56852468	4.64257407	2.34295500
C	2.89212688	0.67001520	0.75996276
C	0.95817134	1.89101887	1.13255458
H	-0.13205551	1.92638478	1.07264142
C	3.09641931	2.80803223	1.55525866
C	-2.25482854	-3.06036213	0.85503219
H	-1.98150096	-3.05980994	1.91863367
H	-2.77003118	-3.99908908	0.60462323
H	-2.90318692	-2.19751977	0.64804134
C	1.68981506	2.96736601	1.54831008
H	1.20011044	3.88548827	1.87291929
C	8.78737018	1.06894668	1.49034477
H	8.51875298	1.88698035	0.80856960
H	9.88001478	1.03039797	1.60642087
H	8.32019070	1.24834416	2.46797970
C	0.24808245	-4.40034333	0.19464434
H	-0.34159468	-5.30228825	-0.02269122
H	0.54804106	-4.39696321	1.25092453
H	1.15394208	-4.38922132	-0.42617218
C	8.79286627	-1.79898809	1.95570022
H	8.32347366	-1.66528897	2.93945322
H	9.88546499	-1.72192884	2.05197652
H	8.52514333	-2.79119999	1.56857198
C	9.11594840	-0.76357177	-0.74066283
H	8.85260678	-1.73804483	-1.17319913
H	10.19526250	-0.73122922	-0.53329204
H	8.85314141	0.02502265	-1.45825087
C	-1.29233269	-3.08289203	-1.88788243
H	-1.93235231	-2.23168860	-2.15615893
H	-1.84809909	-4.02360801	-2.00912622
H	-0.41460433	-3.08832159	-2.54766756
Au	-5.74604047	0.07829209	0.84823853
Au	-1.00143163	0.75181665	-1.86996835
S	-3.04711762	0.30521591	-0.78022771
P	-7.32955830	-1.54858059	0.62053543
P	0.90138967	1.09071478	-3.13241986
N	-4.35428249	1.62745412	1.07704504
N	-2.33826403	2.62084668	0.36050928
N	-1.61584995	4.61923947	1.18437128
H	-0.96542356	4.62771013	0.40870667
H	-1.80972327	5.50045169	1.63994285
C	-3.23522080	1.64944872	0.31219003
C	-4.54831107	2.65078698	1.93068665
H	-5.45338592	2.60597322	2.53862896
C	-2.54786987	3.65163408	1.18495924
C	-8.67210664	-1.08968638	-0.53672874
H	-8.24263115	-0.87360015	-1.52399000
H	-9.39585924	-1.91327908	-0.61828544
H	-9.17829252	-0.18906667	-0.16458775
C	-3.67488843	3.69693430	2.03181556

H	-3.85786832	4.51963858	2.72291747
C	0.53706801	1.62549909	-4.84819574
H	-0.02667236	2.56755890	-4.82334080
H	1.47160374	1.76656945	-5.41009038
H	-0.07805555	0.86111178	-5.34146414
C	-6.64497683	-3.11796459	-0.03382018
H	-7.44513479	-3.86376304	-0.14383860
H	-6.18031581	-2.92684072	-1.01046655
H	-5.88182248	-3.49544215	0.65993254
C	1.94851081	-0.40131693	-3.30960041
H	1.35027705	-1.21049836	-3.74888151
H	2.80681632	-0.18343526	-3.96131669
H	2.30949089	-0.70683782	-2.31650630
C	2.03483154	2.37543503	-2.47804492
H	2.38759983	2.07532083	-1.48385585
H	2.89609638	2.49156426	-3.15114204
H	1.49676686	3.32915139	-2.39973028
C	-8.16660431	-1.99976379	2.18510989
H	-8.66699426	-1.11271286	2.59578460
H	-8.90908269	-2.78916536	2.00012799
H	-7.42083365	-2.35432926	2.90888662

Table S17. Cartesian coordinates of the optimized structure of model **4b** (DFT-D3/PBE).

C	1.86871300	-2.13312000	1.06245400
C	4.13748400	-2.46654500	0.86349300
C	4.05532000	-2.28165100	-0.53530700
C	2.81777800	-2.00804900	-1.03453200
N	1.70782600	-1.93138100	-0.26464700
N	3.04278600	-2.37936500	1.62524600
N	5.29170600	-2.72654500	1.47447700
S	0.55620600	-2.12025600	2.24119200
C	-3.42981700	-1.12144900	-1.06274100
S	-2.16340600	-1.38712700	-2.26066000
C	-4.30732900	-0.89088300	1.05913900
C	-5.55357800	-0.65673400	0.56190700
C	-5.67560500	-0.66733100	-0.84621400
N	-6.83385900	-0.42244100	-1.45593300
N	-3.22877600	-1.12806400	0.27651100
N	-4.61163200	-0.90600700	-1.61926400
Au	-0.11529200	-1.57340800	-1.22209600
Au	-1.42470600	-1.56958000	1.21591500
H	-4.11940500	-0.89196200	2.13327100
H	-6.39679600	-0.45538000	1.22151400
H	4.92888600	-2.33382800	-1.18439800
H	2.66602600	-1.82602900	-2.09858200
H	6.15909600	-2.76388700	0.95971700
H	5.31272500	-2.81159600	2.48161300
H	-6.88239400	-0.46634400	-2.46489900
H	-7.68224200	-0.27393000	-0.92939900
C	-1.86872600	2.13298700	1.06261300
C	-4.13748200	2.46651600	0.86366500
C	-4.05530500	2.28180100	-0.53515800
C	-2.81776500	2.00822700	-1.03440300
N	-1.70782700	1.93141900	-0.26451300
N	-3.04279800	2.37920100	1.62542200
N	-5.29170300	2.72648000	1.47466700
S	-0.55624100	2.11990400	2.24137300
C	3.42983100	1.12158300	-1.06265200
S	2.16341500	1.38732100	-2.26055200
C	4.30734300	0.89086400	1.05921000
C	5.55359900	0.65678600	0.56196200
C	5.67562900	0.66750500	-0.84615700
N	6.83389200	0.42270000	-1.45589400
N	3.22878700	1.12808200	0.27659900
N	4.61165300	0.90622100	-1.61919000
Au	0.11529500	1.57351100	-1.22198300
Au	1.42469500	1.56943200	1.21603500
H	4.11941700	0.89185400	2.13334200
H	6.39682000	0.45540200	1.22155600
H	-4.92886100	2.33409100	-1.18425400
H	-2.66600600	1.82635700	-2.09847700
H	-6.15908500	2.76391700	0.95990200
H	-5.31273300	2.81139700	2.48181500
H	6.88242800	0.46669000	-2.46485700
H	7.68227800	0.27416200	-0.92937200

Table S18. Cartesian coordinates of the optimized structure of model **4c** (DFT-D3/PBE).

Au	0.01332600	2.05333300	-0.23147000
Au	2.05334700	-0.01333000	0.23147100
Au	-2.05334700	0.01333000	0.23147100
Au	-0.01332600	-2.05333300	-0.23147000
C	1.13248700	1.40884700	2.84097900
C	2.24046600	-0.60263200	3.08916700
C	1.06568200	1.48986000	4.22203700
H	2.70446000	-1.45720900	2.59117700
C	1.63775400	0.46400600	4.98701800
H	0.56311500	2.33184900	4.69820800
C	0.60258700	2.24049200	-3.08916300
C	-1.40886700	1.13246600	-2.84098200
H	1.45715000	2.70451100	-2.59117300
C	-1.48987200	1.06565600	-4.22203900
C	-0.46402600	1.63774800	-4.98701800
H	-2.33185000	0.56307300	-4.69821300
C	-2.24046600	0.60263200	3.08916700
C	-1.13248700	-1.40884700	2.84097900
H	-2.70446000	1.45720900	2.59117700
C	-1.06568200	-1.48986000	4.22203700
C	-1.63775400	-0.46400600	4.98701800
H	-0.56311500	-2.33184900	4.69820800
C	-0.60258700	-2.24049200	-3.08916300
C	1.40886700	-1.13246600	-2.84098200
C	1.48987200	-1.06565600	-4.22203900
C	0.46402600	-1.63774800	-4.98701800
H	2.33185000	-0.56307300	-4.69821300
S	-2.74039900	0.46398400	-1.92035800
S	-0.46402600	-2.74038700	1.92035100
S	2.74039900	-0.46398400	-1.92035800
S	0.46402600	2.74038700	1.92035100
H	-1.45715000	-2.70451100	-2.59117300
N	1.74006000	0.33435100	2.26780700
N	-1.74006000	-0.33435100	2.26780700
N	0.33438300	-1.74006400	-2.26780800
N	-0.33438300	1.74006400	-2.26780800
N	0.59607800	2.23026200	-4.39423100
N	2.23023800	-0.59611700	4.39423300
N	-2.23023800	0.59611700	4.39423300
N	-0.59607800	-2.23026200	-4.39423100
N	0.47258500	-1.62536900	-6.32042100
N	-0.47258500	1.62536900	-6.32042100
N	-1.62538900	-0.47257200	6.32042100
N	1.62538900	0.47257200	6.32042100
H	-1.97995800	0.33268000	6.81791800
H	-1.12870900	-1.18488900	6.83493200
H	1.12870900	1.18488900	6.83493200
H	1.97995800	-0.33268000	6.81791800
H	1.18491900	-1.12871900	-6.83493600
H	-0.33263100	-1.98001000	-6.81792500
H	0.33263100	1.98001000	-6.81792500
H	-1.18491900	1.12871900	-6.83493600